

# Distribution amplitudes of heavy-light pseudo-scalar and vector mesons from Dyson-Schwinger equations framework

---

Yin-Zhen Xu

*Departamento de Ciencias Integradas, Universidad de Huelva,  
E-21071 Huelva, Spain*

*Departamento de Sistemas Físicos, Químicos y Naturales, Universidad Pablo de Olavide,  
E-41013 Sevilla, Spain*

*E-mail:* [yinzhen.xu@dc1.uhu.es](mailto:yinzhen.xu@dc1.uhu.es)

ABSTRACT: We systematically investigate leading-twist distribution amplitudes of ground state heavy-light pseudo-scalar and vector mesons, the results of  $B^*$ ,  $B_s^*$ ,  $B_c^*$  mesons are reported for the first time within the Dyson-Schwinger equations framework. A novel numerical method for calculating Mellin moments is proposed, which can avoid extrapolation or fitting in previous similar studies. Based on it, we calculate the first eight Mellin moments of mesons and reconstruct their distribution amplitudes. It is found that, in flavor-asymmetric systems, distribution amplitude  $\phi(x)$  is skewed to one side, with the position of the maximum  $\sim M_E^f/(M_E^f + M_E^g)$ , where  $M_E$  is Euclidean constituent quark mass and  $f/g$  denote the flavor of heavier/lighter quark in the meson, respectively. For systems with the same valence quark structure, the first Mellin moments follow the relation  $\langle \xi \rangle_{0^-} < \langle \xi \rangle_{1^-}^{\parallel} < \langle \xi \rangle_{1^-}^{\perp}$ , where  $\xi = 2x - 1$  and  $x$  is the momentum fraction carried by the heavier quark. Our predictions can be compared with experimental data and further theoretical calculations in the future, and the results of light mesons such as  $\pi$ ,  $K$ ,  $\rho$  are consistent with recent lattice data.

---

## Contents

|          |   |           |
|----------|---|-----------|
| <b>1</b> | <b>Introduction</b>                                       | <b>1</b>  |
| <b>2</b> | <b>Distribution amplitudes within DSEs/BSEs framework</b> | <b>2</b>  |
| 2.1      | Quark propagators in the complex plane                    | 2         |
| 2.2      | Meson's BSAs in two-dimensional Chebyshev tensor grid     | 4         |
| 2.3      | Distribution amplitudes and Mellin moments                | 8         |
| <b>3</b> | <b>Numerical results and discussion</b>                   | <b>10</b> |
| 3.1      | Mellin moments  | 10        |
| 3.2      | Distribution amplitudes                                   | 13        |
| <b>4</b> | <b>Summary and Perspectives</b>                           | <b>17</b> |
| <b>A</b> | <b>Fitting DAs based on Mellin moments</b>                | <b>17</b> |

---

## 1 Introduction

The study of meson is a fundamental topic in hadron physics. Meson's leading-twist distribution amplitudes (DAs), typically defined as the matrix element of non-local operators between meson state and the vacuum, describe the longitudinal momentum distribution of valence quark in the limit of negligible transverse momentum [1–3]. Meanwhile, they are also important inputs in many hard exclusive processes at large momentum transfers and play a central role in QCD factorization theory [4, 5]. In the asymptotic limit, it is well-known that pion's DAs follow a simple form,  $\phi^{\text{asy}}(x) = 6x(1-x)$  [6]. However, their shapes at hadronic scales are non-perturbative and therefore pose a theoretical challenge [7].

In the past few decades, the DAs of meson have attracted growing attention and different methods have been applied, for example, lattice QCD (lQCD) [8–15], QCD sum rule (SR) [16–20], Heavy Quark Effective Theory (HQET) [21–23], Algebraic model (AM) [24, 25], light-front quark model (LFQM) [26–29] and Dyson-Schwinger/Bethe-Salpeter equations framework (DSEs/BSEs) [30–41]. In these approaches, the DSEs/BSEs formalism, which provides a non-perturbative and Poincaré-covariant framework capable of simultaneously describing confinement and dynamical chiral symmetry breaking (DCSB), has been successfully used to study hadron properties for thirty years [41–68]. Compared with light mesons, heavy-light systems exhibit higher flavor asymmetry, thereby offering more information for the internal structure of QCD's bound states. In particular, their DAs are important theoretical inputs in the studies of some decay such as  $B \rightarrow K^* \ell^+ \ell^-$ ,  $B_s \rightarrow \phi \ell^+ \ell^-$ , which may aid in exploring new physics beyond the standard model [69–71].

Recently, with significant progress in exploring the properties of heavy-light mesons within the DSEs/BSEs framework [38, 40, 41, 52, 55, 57, 60, 63, 67], the corresponding investigations of meson DAs within this framework have been extended from flavor-symmetric or slightly asymmetric cases [30–36, 39] to heavy-light structures [37, 38, 40, 41].

On the other hand, meson DAs can be expressed as the light-front projection of the Bethe-Salpeter wave function and reconstructed from Mellin moments [30]. However, due to the highly multi-dimensional oscillatory integrand, it is difficult to obtain these moments directly from Bethe-Salpeter amplitudes (BSAs), especially for light mesons [34, 35]. Instead, there are two common ways to estimate them. The fitting method is applied first:  $n$  complex-conjugate pole parameterizations/Nakanishi representations are considered as an ansatz to fit the numerical solution of the quark propagator/BSAs [30, 38], allowing the integral to be processed analytically. However, fitting parameters up to a few dozen will introduce ambiguity [40]. Subsequently, a factor  $1/(1+k^2r^2)^m$  is introduced to suppress oscillations, aiming for direct computation by extrapolating  $r^2 \rightarrow 0$  [34–36]. For pion, this method can reach the fourth moment [39].

In this work, building on our previous studies of heavy-light pseudo-scalar and vector mesons [60, 63], we systematically calculate the first eight Mellin moments and reconstruct their DAs. These moments are extracted from the BSAs by utilizing the two-dimensional Chebyshev tensor grid (CTG) [72, 73] and the multi-dimensional adaptive integration algorithm [74–77], thereby eliminating the need for extrapolation or fitting as employed in previous similar studies. The results of  $B^*$ ,  $B_s^*$ ,  $B_c^*$  mesons are reported for the first time and our predictions for light mesons such as  $\pi$ ,  $K$ ,  $\rho$  are consistent with recent lattice data.

This paper is organized as follows: In section 2, we introduce the DSEs/BSEs framework and meson DAs. In section 3, the numerical results of heavy-light pseudo-scalar/vector meson DAs are presented. Then we discuss the effect of flavor symmetry breaking, and the results are compared with those obtained from other approaches. Section 4 provides a brief summary and perspectives.

## 2 Distribution amplitudes within DSEs/BSEs framework

### 2.1 Quark propagators in the complex plane

We work within the DSEs/BSEs framework in Euclidean space. As a first step, the dressed-quark propagator is obtained from the following gap equation:

$$S^{-1}(k) = Z_2 i\gamma \cdot k + Z_4 m + Z_1 \int^{\Lambda} \frac{d^4q}{(2\pi)^4} g^2 D_{\mu\nu}(k-q) \frac{\lambda^a}{2} \gamma_\mu S(q) \frac{\lambda^a}{2} \Gamma_\nu(k, q), \quad (2.1)$$

and the general form of  $S^{-1}(k)$  is

$$S^{-1}(k) = i\gamma \cdot p A(k^2) + B(k^2). \quad (2.2)$$

Where  $A(k^2)$  and  $B(k^2)$  are scalar functions,  $m$  is current-quark mass,  $Z_{1,2,4}$  are the renormalization constants,  $\Lambda$  represents a regularization scale. In this work we employ a mass-independent momentum-subtraction renormalisation scheme and choose renormalization

scale  $\zeta = 2$  GeV [36, 48, 56]. The quark mass function  $\tilde{M}(k^2) = B(k^2)/A(k^2)$  is independent of  $\zeta$  and the renormalisation-group invariant current-quark mass can be defined by [47, 57]

$$\hat{m} = \lim_{k^2 \rightarrow \infty} \left[ \frac{1}{2} \ln \frac{k^2}{\Lambda_{\text{QCD}}^2} \right]^{\gamma_m} \tilde{M}(k^2), \quad (2.3)$$

accordingly, one-loop evolved current-quark mass reads [43, 57]

$$m^\zeta = \hat{m} / \left[ \frac{1}{2} \ln \frac{\zeta^2}{\Lambda_{\text{QCD}}^2} \right]^{\gamma_m}. \quad (2.4)$$

Another quantity that can be obtained from the quark mass function is the Euclidean constituent quark mass [44]

$$M_E = \left\{ k \mid k^2 = \tilde{M}^2(k^2) \right\}, \quad (2.5)$$

which provides a realistic estimate of the quark's active quasi-particle mass [53, 78].

In conjunction with dressed quark-gluon vertex  $\Gamma_\nu(k, q) \rightarrow Z_2 \gamma_\nu$  [79], which characterizes the rainbow-ladder (RL) truncation, we adopt the following form for the gluon propagator:

$$Z_1 g^2 D_{\mu\nu}(l) \Gamma_\nu(k, q) = Z_2^2 \mathcal{G}(l^2) \mathcal{P}_{\mu\nu}^T(l) \gamma_\nu = \mathcal{D}_{\text{eff}} \gamma_\nu, \quad (2.6)$$

where  $l = k - q$ ,  $\mathcal{P}_{\mu\nu}^T(l) = \delta_{\mu\nu} - l_\mu l_\nu / l^2$  is transverse projection operator, and the effective interaction is chosen as the Qin-Chang model [49, 51]

$$\frac{\mathcal{G}(l^2)}{l^2} = \mathcal{G}^{\text{IR}}(l^2) + \frac{8\pi^2 \gamma_m \mathcal{F}(l^2)}{\ln[\tau + (1 + l^2/\Lambda_{\text{QCD}}^2)^2]}, \quad \mathcal{G}^{\text{IR}}(l^2) = D \frac{8\pi^2}{\omega^4} e^{-l^2/\omega^2}. \quad (2.7)$$

with  $\mathcal{F}(l^2) = \{1 - \exp[-l^2/(4m_t^2)]\}/l^2$ ,  $m_t = 0.5$  GeV,  $\tau = e^2 - 1$ ,  $\Lambda_{\text{QCD}} = 0.234$  GeV,  $\gamma_m = 12/25$  [80]. For the infrared model parameters, in line with refs. [41, 60, 63] we choose  $(D\omega)_{u/d} = (0.82 \text{ GeV})^3$ ,  $(D\omega)_s = (0.68 \text{ GeV})^3$ ,  $(D\omega)_c = (0.66 \text{ GeV})^3$ ,  $(D\omega)_b = (0.48 \text{ GeV})^3$ , with  $\omega_{u/d,s} = 0.5$  GeV,  $\omega_{c,b} = 0.8$  GeV. More details of eq. (2.1-2.7) are presented in refs. [42, 44–46, 49].

In the calculation of bound states, arising from the on-shell condition  $P^2 = -M^2$ , the dressed-quark propagator  $S(k_\pm)$  is often obtained by solving eq. (2.1) in the complex plane [81, 82]. Here,  $M$  denotes the meson mass,  $k_\pm = k \pm \alpha_\pm P$ ,  $\alpha_+ = \alpha$ ,  $\alpha_- = 1 - \alpha$ , and  $\alpha \in [0, 1]$  represents the momentum partitioning parameter. In this work, we adopt the common rest frame

$$k = (0, 0, \sin \theta, \cos \theta) |k|, \quad P = (0, 0, 0, iM), \quad (2.8)$$

correspondingly, the value of  $k_\pm^2$  is constrained by the following parabola

$$\text{Re}(k_\pm^2) = -\alpha_\pm^2 M^2 + \frac{\text{Im}^2(k_\pm^2) \sec^2 \theta}{4M^2 \alpha_\pm^2}, \quad \theta \in [0, \pi]. \quad (2.9)$$

Although the physical observables do not depend on  $\alpha$ , in the actual calculation, the selection of  $\alpha$  should be made carefully to avoid the parabola including the pole for the accuracy

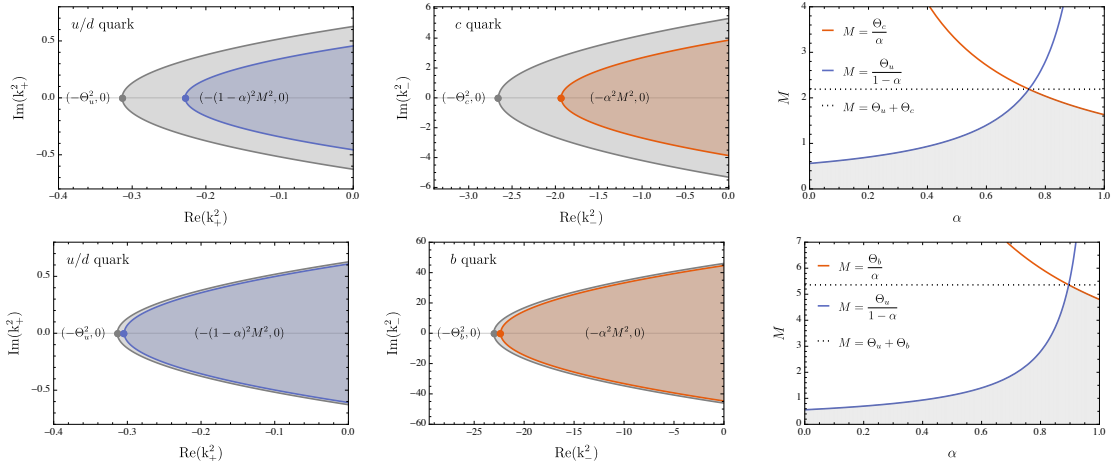


**Figure 1.** This figure illustrates the adjustment of  $\alpha$  using the  $D$  meson (upper panels) and  $B$  meson (lower panels) as examples. In the left and middle panels, the gray area denotes the computable region when  $\text{Re}(k_{\perp}^2) < 0$ , while the colored area indicates the region required for calculating  $D$  and  $B$  mesons with optimal  $\alpha$ . In the right panels, the gray area represents the range of meson masses that can be computed as  $\alpha$  varies (see eq. (2.10)).

of the contour integral [81, 83] (see figure 1, left and middle panels). If we define the vertex of parabola as  $(-\Theta^2, 0)$ , the momentum partitioning parameter  $\alpha$  should satisfy the following relation [63]

$$1 - \Theta_{\bar{g}}/M < \alpha < \Theta_f/M. \quad (2.10)$$

Furthermore, the maximum computable mass is given by  $\Theta_f + \Theta_{\bar{g}}$ , and the corresponding  $\alpha$ , namely, the optimal  $\alpha = \Theta_f/(\Theta_f + \Theta_{\bar{g}})$  [82] (see figure 1, right panels). In this work, we obtain  $\Theta_u = 0.56$  GeV,  $\Theta_s = 0.67$  GeV,  $\Theta_c = 1.63$  GeV,  $\Theta_b = 4.8$  GeV. As long as the quark propagator on the parabola is determined, its value at any interior point of the parabola can be directly obtained through the Cauchy integral theorem [84].

## 2.2 Meson's BSAs in two-dimensional Chebyshev tensor grid

The next step is the meson's Bethe-Salpeter amplitudes (BSAs). Generically, those can be calculated based on the following homogeneous BSEs

$$\Gamma_H^{f\bar{g}}(P; k^2, k \cdot P) = \int^{\Lambda} \frac{d^4 q}{(2\pi)^4} K^{f\bar{g}}(q, k; P) S^f(q_+) \Gamma_H^{f\bar{g}}(P; q^2, q \cdot P) S^g(q_-), \quad (2.11)$$

with  $f$  and  $g$  denote the flavor of (anti-)quark, and the corresponding quark propagators have been discussed in the last subsection. In the standard RL approximation, the interaction kernel is given by [80]

$$K^{f\bar{g}}(q, k; P) = \tilde{\mathcal{D}}_{\text{eff}}^{f\bar{g}} \frac{\lambda^a}{2} \gamma_{\mu} \otimes \frac{\lambda^a}{2} \gamma_{\nu}, \quad \tilde{\mathcal{D}}_{\text{eff}}^{f\bar{g}} = \mathcal{D}_{\text{eff}}^f, \quad (2.12)$$

where  $\mathcal{D}_{\text{eff}}^f$ , defined by eq. (2.6), describes the strength of interaction and decreases as the mass of quark increases because the dressed-effect is suppressed [52, 100]. Over the

| Meson      | Mass [GeV] |           |                    | Decay constant [GeV] |           |           |
|------------|------------|-----------|--------------------|----------------------|-----------|-----------|
|            | Expt.      | lQCD      | This work          | Expt.                | lQCD      | This work |
| $\pi$      | 0.138(1)   | -         | 0.135              | 0.092(1)             | 0.093(1)  | 0.095     |
| $\rho$     | 0.775(1)   | 0.780(16) | 0.755              | 0.153(1)             | -         | 0.150     |
| $\phi$     | 1.019(1)   | 1.032(16) | 1.019              | 0.168(1)             | 0.170(13) | 0.168     |
| $\eta_c$   | 2.984(1)   | -         | 2.984              | 0.237(52)            | 0.278(2)  | 0.270     |
| $J/\psi$   | 3.097(1)   | 3.098(3)  | 3.114              | 0.294(5)             | 0.286(4)  | 0.290     |
| $\eta_b$   | 9.399(1)   | -         | 9.399              | -                    | 0.472(5)  | 0.464     |
| $\Upsilon$ | 9.460(1)   | -         | 9.453              | 0.505(4)             | 0.459(22) | 0.441     |
| $K$        | 0.495(1)   | -         | 0.495 <sup>†</sup> | 0.110(1)             | -         | 0.108     |
| $K^*$      | 0.896(1)   | 0.993(1)  | 0.880              | 0.159(1)             | -         | 0.158     |
| $D$        | 1.868(1)   | 1.868(3)  | 1.868 <sup>†</sup> | 0.144(4)             | 0.150(4)  | 0.140     |
| $D^*$      | 2.009(1)   | 2.013(14) | 2.017              | -                    | 0.158(6)  | 0.160     |
| $D_s$      | 1.968(1)   | 1.968(4)  | 1.968 <sup>†</sup> | 0.182(3)             | 0.177(1)  | 0.164     |
| $D_s^*$    | 2.112(1)   | 2.116(11) | 2.111              | -                    | 0.190(5)  | 0.186     |
| $B$        | 5.279(1)   | 5.283(8)  | 5.279 <sup>†</sup> | 0.133(18)            | 0.134(1)  | 0.123     |
| $B^*$      | 5.325(1)   | 5.321(8)  | 5.334              | -                    | 0.131(5)  | 0.126     |
| $B_s$      | 5.367(1)   | 5.366(8)  | 5.367 <sup>†</sup> | -                    | 0.163(1)  | 0.149     |
| $B_s^*$    | 5.415(1)   | 5.412(6)  | 5.422              | -                    | 0.158(4)  | 0.151     |
| $B_c$      | 6.275(1)   | 6.276(7)  | 6.275 <sup>†</sup> | -                    | 0.307(10) | 0.300     |
| $B_c^*$    | -          | 6.331(7)  | 6.340              | -                    | 0.298(9)  | 0.296     |

**Table 1.** The masses and decay constants of mesons, with renormalization-group-invariant current-quark mass (see eq. (2.3)):  $\hat{m}_{u/d} = 0.0068$  GeV,  $\hat{m}_s = 0.198$  GeV,  $\hat{m}_c = 1.739$  GeV,  $\hat{m}_b = 7.494$  GeV; one-loop evolved current-quark mass in 2 GeV (see. eq. (2.4)):  $m_{u/d}^{\zeta_2} = 0.0047$  GeV,  $m_s^{\zeta_2} = 0.137$  GeV,  $m_c^{\zeta_2} = 1.205$  GeV,  $m_b^{\zeta_2} = 5.195$  GeV; Euclidean constituent quark mass (see eq. (2.5)):  $M_E^{u/d} = 0.423$  GeV,  $M_E^s = 0.489$  GeV,  $M_E^c = 1.333$  GeV,  $M_E^b = 4.256$  GeV, and <sup>†</sup> denote the fitting values from weight factor (see eq. (2.13)). For comparison, we collect both experimental values [85, 86] and lQCD's results [87–99].

past thirty years, eq. (2.12) has been widely used in flavor symmetric/slightly asymmetric systems such as  $u\bar{d}$ ,  $u\bar{s}$ ,  $c\bar{c}$ . However, for heavy-light meson, the RL kernel is difficult to be applied due to the lack of flavor asymmetry. Accordingly, different effective kernels have been developed [38, 40, 55, 57, 61]. In this work, we apply the so-called weight-RL approximation, that is, arithmetically average the RL kernels for different flavors as [41, 52, 60, 63]

$$\tilde{\mathcal{D}}_{\text{eff}}^{f\bar{g}} = \eta \mathcal{D}_{\text{eff}}^f + (1 - \eta) \mathcal{D}_{\text{eff}}^{\bar{g}}. \quad (2.13)$$

Where a weight factor  $\eta$  is introduced and in the case of flavor-symmetric mesons, it will degenerate to the RL kernel. For flavor-asymmetric mesons, the effect of weight factor has been discussed in ref. [52], with an automatic averaging presented. In line with refs. [41, 60, 63], we directly determine  $\eta$  by the pseudo-scalar meson's mass to obtain a relatively realistic interaction. After the weight factor is fixed, the decay constant of the pseudo-scalar meson, the mass and decay constant of the vector meson can all be well predicted (see table 1). It is worth noting that, under a strict heavy-light kernel, once the flavor-dependence of interaction is determined in gap equation, fitting for heavy-light mesons is not required. Therefore, the weight factor in this kernel ansatz should be considered as a cost of calculating heavy-light mesons in the RL framework, to remedy the effects of flavor

asymmetry in BSEs. The theoretical explore for flavor dependence and strict beyond-RL kernel is still ongoing and remains highly challenging [55, 57, 67, 68, 82, 101–103].

The general form of  $\Gamma(P; k^2, k \cdot P)$  is given by

$$\Gamma(P; k^2, k \cdot P) = \sum_{i=1}^N \tau^i(k, P) \mathcal{F}_i(k, P), \quad (2.14)$$

where  $\tau^i(k, P)$  is basis and  $\mathcal{F}_i(k, P)$  is scalar function. For the pseudo-scalar/vector meson, we choose [51]

$$\begin{aligned} \tau_{0-}^1 &= i\gamma_5, & \tau_{0-}^3 &= \gamma_5 \gamma \cdot k k \cdot P, \\ \tau_{0-}^2 &= \gamma_5 \gamma \cdot P, & \tau_{0-}^4 &= \gamma_5 \sigma_{\mu\nu} k_\mu P_\nu, \end{aligned} \quad (2.15a)$$

and

$$\begin{aligned} \tau_{1-}^1 &= i\gamma_\mu^T, & \tau_{1-}^5 &= k_\mu^T, \\ \tau_{1-}^2 &= i [3k_\mu^T \gamma \cdot k^T - \gamma_\mu^T k^T \cdot k^T], & \tau_{1-}^6 &= k \cdot P [\gamma_\mu^T \gamma^T \cdot k - \gamma \cdot k^T \gamma_\mu^T], \\ \tau_{1-}^3 &= ik_\mu^T k \cdot P \gamma \cdot P, & \tau_{1-}^7 &= (k^T)^2 (\gamma_\mu^T \gamma \cdot P - \gamma \cdot P \gamma_\mu^T) - 2k_\mu^T \gamma \cdot k^T \gamma \cdot P, \\ \tau_{1-}^4 &= i [\gamma_\mu^T \gamma \cdot P \gamma \cdot k^T + k_\mu^T \gamma \cdot P], & \tau_{1-}^8 &= k_\mu^T \gamma \cdot k^T \gamma \cdot P, \end{aligned} \quad (2.15b)$$

with  $V_\mu^T = V_\mu - P_\mu(V \cdot P)/P^2$ . Then the decay constant can be obtained easily after normalization of the meson' BSAs [51].

With these in hand, the traditional treatment of eq. (2.11) is to discretize the integral based on quadrature rule, such as Gauss–Legendre. It then reduces to the eigenvalue problem of the matrix, which can be solved by matrix-free iterative methods, for example, Arnoldi iteration implemented by ARPACK library [104]. However, the obtained eigenvector  $\Gamma_H(P; k^2, k \cdot P)$  is therefore discretized on the  $(k^2, z_k)$  plane, where  $z_k = k \cdot P/(|k| \cdot |P|)$ . This prompts us to look for a reasonable way to make them continuous.

In approximation theory, the Chebyshev series converges for any function that is Lipschitz continuous on  $[-1, 1]$ , and the interpolation polynomial based on Chebyshev nodes provides an approximation that is close to the best polynomial approximation to a continuous function under the maximum norm. In the multidimensional case, the tensor products of Chebyshev node, namely, Chebyshev tensor grid (CTG), have been widely used for function reconstruction [72, 73, 105, 106]. Consider a continuous smooth bivariate  $f : [-1, 1]^2 \rightarrow \mathbb{R}$  which can be expanded as

$$f(x, y) = \sum_{i=0}^{\infty} \sum_{j=0}^{\infty} c_{ij} T_i(x) T_j(y), \quad (2.16)$$

where  $T_n(x)$  is the first kind of Chebyshev polynomial. According to discrete orthogonality condition

$$\sum_{k=0}^{N-1} T_i(x_k) T_j(x_k) = \frac{N}{2 - \delta_{0i}} \delta_{ij}, \quad (2.17)$$

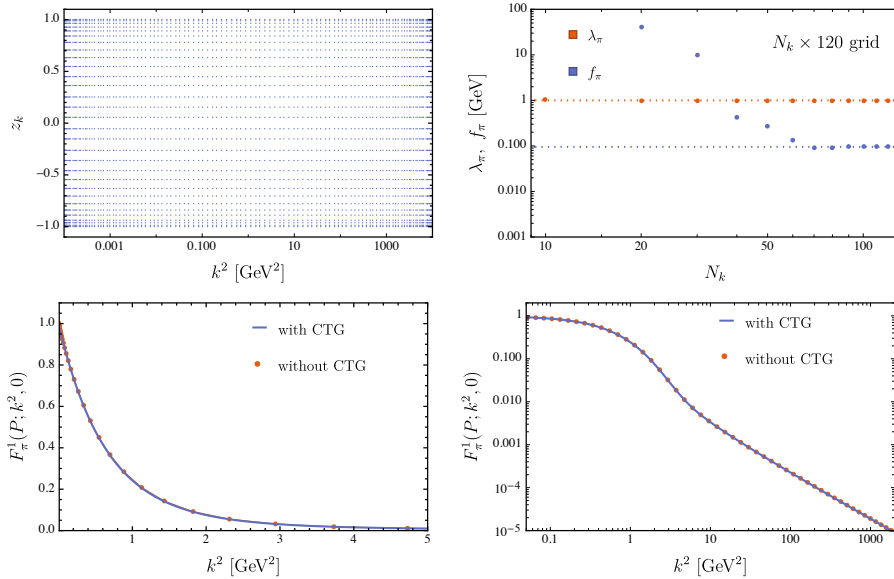


**Figure 2.** The upper left panel presents an example of  $N_k \times N_{z_k}$  CTG, where  $N_{z_k} = 30$  denotes the number of angular nodes and  $N_k = 120$  represents the exponentially mapped radial nodes. The upper right panel shows that as the number of CTG nodes increases, the eigenvalue  $\lambda$  and decay constant  $f$  of the pion gradually stabilize, approaching the constant values indicated by the dotted lines, which represent results from the traditional method. The lower panels further compare the dominant BSA of the pion (without normalization) obtained using these two approaches.

this series can be truncated as

$$\begin{aligned}
 f(x, y) &\simeq \sum_{i=0}^{N_x-1} \sum_{j=0}^{N_y-1} \tilde{c}_{ij} T_i(x) T_j(y), \\
 \tilde{c}_{ij} &= \frac{2 - \delta_{0i}}{N_x} \frac{2 - \delta_{0j}}{N_y} \sum_{k=0}^{N_x-1} \sum_{k'=0}^{N_y-1} f(x_k, y_{k'}) T_i(x_k) T_j(y_{k'}),
 \end{aligned} \tag{2.18}$$

where  $(x_k, y_{k'})$  is the Chebyshev nodes in  $N_x \times N_y$  grid

$$(x_k, y_{k'}) = \left( \cos \left( \frac{2k+1}{2N_x} \pi \right), \cos \left( \frac{2k'+1}{2N_y} \pi \right) \right), k = 0, \dots, N_x - 1; k' = 0, \dots, N_y - 1. \tag{2.19}$$

Therefore, the continuous two-dimensional (2D) function can be obtained once  $f(x_k, y_{k'})$ , the function values on the nodes grid, are known.

Based on it, we map the original  $[-1, 1]^2$  grid to the actual range we need (see figure 2, upper left panel), and then iterate eq. (2.11) on this grid, that is, updating the BSAs on the Chebyshev nodes each time. As the number of nodes increases, the results converge gradually to those of the traditional method (see figure 2, upper right panel). Furthermore, in figure 2, lower panels, we compare the BSAs of pion with and without CTG, it is found that both are consistent in infrared and ultraviolet region. In this work, we apply  $240 \times 120$  CTG and the continuous BSAs obtained will be used to the calculation of DAs in next subsection.



### 2.3 Distribution amplitudes and Mellin moments

In the DSEs/BSEs framework, the meson distribution amplitudes  $\phi(x)$  can be reconstructed through the Mellin moments defined as  $\langle x^m \rangle = \int_0^1 dx x^m \phi(x)$  [30]. For the pseudo-scalar meson (PS), these moments are given by [30, 38]

$$\langle x^m \rangle = \frac{Z_2 N_c}{f_{0^-}} \text{Tr}_D \int^\Lambda \frac{d^4 k}{(2\pi)^4} \frac{(n \cdot k_+)^m}{(n \cdot P)^{m+1}} \gamma_5 \gamma \cdot n \chi(k, P), \quad (2.20a)$$

and for vector meson (VC), the longitudinally and transversely polarized moments read [39, 40]

$$\langle x^m \rangle_{\parallel} = \frac{M_{1^-} N_c Z_2}{f_{1^-}} \text{Tr}_D \int^\Lambda \frac{d^4 k}{(2\pi)^4} \frac{(n \cdot k_+)^m}{(n \cdot P)^{m+2}} \gamma \cdot n n_\nu \chi_\nu(k, P), \quad (2.20b)$$

$$\langle x^m \rangle_{\perp} = -\frac{N_c Z_T}{2f_{1\perp}} \text{Tr}_D \int^\Lambda \frac{d^4 k}{(2\pi)^4} \frac{(n \cdot k_+)^m}{(n \cdot P)^{m+1}} n_\mu \sigma_{\mu\rho} \mathcal{O}_{\rho\nu}^\perp \chi_\nu(k, P). \quad (2.20c)$$

Where  $M$  is meson's mass with on-shell condition  $M^2 = -P^2$ , tensor  $\mathcal{O}_{\rho\nu}^\perp = \delta_{\rho\nu} + n_\rho \bar{n}_\nu + \bar{n}_\rho n_\nu$ ,  $\chi_H(k, P)$  denotes the BS wave function, derived from the dressed-quark propagators and BSAs outlined in the preceding subsections:

$$\chi_H(k, P) = S^f(k_+) \Gamma_H(P; k^2, k \cdot P) S^g(k_-), \quad (2.21)$$

with renormalization scale  $\mu = 2$  GeV. In this work, we use the Euclidean metric,  $n = (0, 0, 1, i)$ ,  $\bar{n} = (0, 0, -1/2, i/2)$  is a light-like vector and its conjugate. Finally, the normalization conditions  $\langle x^0 \rangle = 1$  are constrained by decay constants  $f$ ,  $f^\perp$  and renormalization constants  $Z_{2,T}$ . More details and discussion are presented in refs. [30, 38–40].

In principle, once the BS wave function is known, Mellin moments of any order can be evaluated. However, as noted in the introduction, the term  $(n \cdot k_+)^m$  induces highly multi-dimensional oscillations, which makes the numerical computation of eq. (2.20) challenging, especially for light mesons [34, 35]. The rapid development of modern parallel multi-dimensional adaptive integration technology such as CUBA brings forth new opportunities [74, 75], which has been successfully applied to similar oscillatory integral in many fields [107–109]. In the previous subsections, we have obtained continuous quark propagators/BSAs with the help of the Cauchy integral theorem/two-dimensional CTG. Therefore, the CUBA-Cuhre algorithm, a deterministic method grounded in globally adaptive subdivision [76, 77], lends itself naturally to the direct evaluation of eq. (2.20).

Furthermore, continuous BS wave function + CUBA allows us to freely adjust the upper-bound of the momentum integration  $k_{\text{max}}^2$  in eq. (2.20), which is difficult to achieve with traditional approach. In figure 3, upper left panel, we take  $\pi$  as an example to show the variation trend of  $\langle x^m \rangle$  with momentum cutoff. It is found that, with the increase of  $k_{\text{max}}^2$ , the integral value flattens out gradually after a steep raise. Besides, in the actual calculation, it is found that  $\langle x^m \rangle / \langle x^0 \rangle$  can be used to reach the flat region faster (see figure 3, upper right panel).

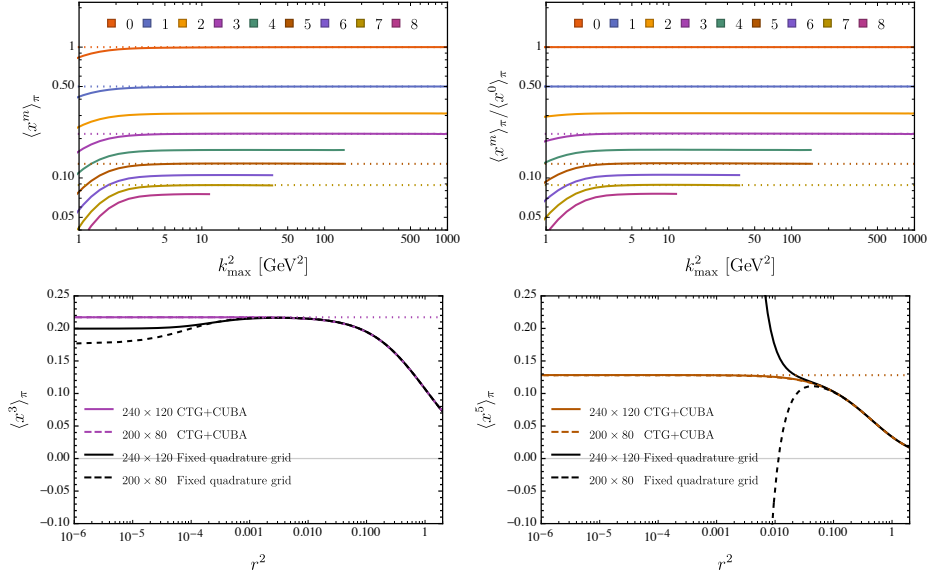


**Figure 3.** The upper panels illustrate the variation of  $\langle x^m \rangle_\pi$  and  $\langle x^m \rangle_\pi / \langle x^0 \rangle_\pi$  with the ultraviolet momentum cutoff  $k_{\max}^2$  in eq. (2.20). Data for higher moments at large cutoffs are absent due to numerical instability. In the lower panels,  $\langle x^3 \rangle_\pi$  and  $\langle x^5 \rangle_\pi$  are used as examples to demonstrate the effect of the damping factor  $1/(1+k^2 r^2)^m$  in two different  $N_k \times N_{z_k}$  CTG. For comparison, results from the traditional fixed quadrature grid are also included. In all panels, the dotted lines indicate the recurrence results (see eq. (2.23)).

For flavor-symmetric ground state pseudo-scalar and vector mesons, their DAs satisfy the following constrain condition [36]

$$\int_0^1 dx x^m \phi(x) = \int_0^1 dx (1-x)^m \phi(x), \quad (2.22)$$

therefore a given odd moment can be expand by all lower even order moments, such as

$$\begin{aligned} \langle x^1 \rangle &= \frac{1}{2}, \quad \langle x^3 \rangle = -\frac{1}{4} + \frac{3}{2} \langle x^2 \rangle, \quad \langle x^5 \rangle = \frac{1}{2} - \frac{5}{2} \langle x^2 \rangle + \frac{5}{2} \langle x^4 \rangle, \\ \langle x^7 \rangle &= -\frac{17}{8} + \frac{21}{2} \langle x^2 \rangle - \frac{35}{4} \langle x^4 \rangle + \frac{7}{2} \langle x^6 \rangle, \dots, \end{aligned} \quad (2.23)$$

which can be used to check the precision of the numerical procedure. In the figure 3, we use the dotted lines to mark the moments obtained by eq. (2.23). When the integral values reach the flat region, our results precisely satisfy the recursion formula.

In order to further verify the reliability of the current results, we also compare them with extrapolation methods. In this approach, a factor  $1/(1+k^2 r^2)^m$  is introduced to suppress the oscillation, then extrapolate to  $r^2 = 0$ , based on the integral value where  $r^2$  is larger than an estimated position [35, 36]. In figure 3, lower panel, we take the  $\langle x^3 \rangle$  and  $\langle x^5 \rangle$  of pion as examples to show how it works. It can be seen that the traditional fixed quadrature grid has failed when  $r^2$  is very small, therefore extrapolation is inevitable. However, CTG + CUBA still remains stable.

### 3 Numerical results and discussion

#### 3.1 Mellin moments

With all the above in hand, the Mellin moments of pseudo-scalar/vector mesons can be computed directly. As mentioned before, these moments are defined by

$$\langle x^m \rangle = \int_0^1 dx x^m \phi(x), \quad (3.1)$$

where  $x$  is the momentum fraction carried by the heavier quark, and it can be readily transformed to

$$\langle \xi^m \rangle = \langle (2x - 1)^m \rangle = \int_0^1 dx (2x - 1)^m \phi(x). \quad (3.2)$$

Besides, another commonly discussed moment is the Gegenbauer moment  $a_n$  [10, 13, 18], which comes from the expansion of DAs using Gegenbauer polynomials

$$\phi(x) = 6x(1-x) \left[ 1 + \sum_{n=1}^{\infty} a_n C_n^{3/2}(2x-1) \right]. \quad (3.3)$$

According to the orthogonality condition

$$\int_0^1 dx C_n^{3/2}(2x-1) C_m^{3/2}(2x-1) 4x(1-x) = \frac{(1+n)(2+n)}{(2n+3)} \delta_{nm}, \quad (3.4)$$

this two moments are related by a simple algebraic relation

$$a_n = \frac{2(2n+3)}{3(n+1)(n+2)} \int_0^1 dx C_n^{3/2}(2x-1) \phi(x), \quad (3.5)$$

particularly, for the first and second moment

$$a_1 = \frac{5}{3} \langle \xi \rangle = -\frac{5}{3} + \frac{10}{3} \langle x \rangle, \quad a_2 = -\frac{7}{12} + \frac{35}{12} \langle \xi^2 \rangle = \frac{7}{3} - \frac{35}{3} \langle x \rangle + \frac{35}{3} \langle x^2 \rangle. \quad (3.6)$$

We first calculate the Mellin moments of the pion and kaon, as they have been relatively well-discussed by various methods. The comparisons of our results for the first and second moments with those from lattice QCD and previous DSE studies are presented in table 2. For  $\langle \xi^2 \rangle_{\pi, K}$ , the results of different approaches are generally consistent, and ours are closer to the latest lattice value than previous DSE results. However, the results of  $\langle \xi \rangle_K$  reported by DSE (RL) are significantly larger, because the interaction kernel strength, fitted to pion properties alone is not optimal in the treatment of heavier quark [56]. Therefore, it is overestimated for kaon and leading to an excessive  $u-s$  quark splitting [32], which is also observed in the gravitational form factors of kaon [59]. In this work, since the weight-RL introduces a suppression for interaction strength from the  $s$  quark, our results are closer to those of lattice and DSE (DB) calculations.

Now we turn our attention to  $\rho$  and  $K^*$  mesons, the valence-quark spin-flip partner of pion and kaon. The results and comparisons are shown in the table 3. For the  $\rho$  meson,

|                    | $\langle \xi^2 \rangle_\pi$ | $\langle \xi \rangle_K$ | $\langle \xi^2 \rangle_K$ |
|--------------------|-----------------------------|-------------------------|---------------------------|
| this work          | 0.246                       | 0.018                   | 0.222                     |
| lattice(20) [12]   | 0.244(30)                   | 0.009(18)               | 0.198(16)                 |
| lattice(19) [11]   | 0.234(6)                    | 0.032(17)               | 0.231(6)                  |
| lattice(11) [8]    | 0.28(2)                     | 0.036(2)                | 0.26(2)                   |
| DSE(21) [39]       | 0.260                       | -                       | -                         |
| DSE(20) [38]       | 0.272(32)                   | 0.124(13)               | 0.234(6)                  |
| DSE(14,RL,DB) [32] | -                           | 0.11,0.04               | 0.24,0.23                 |
| DSE(13,RL,DB) [30] | 0.28,0.25                   | -                       | -                         |

**Table 2.** Compare the first two Mellin moments of  $\pi$  and  $K$  meson with the results of lattice and other DSEs. Where  $\langle \xi^m \rangle$  is defined in eq. (3.2).

|                   | $\langle \xi^2 \rangle_\rho^\parallel$ | $\langle \xi^2 \rangle_\rho^\perp$ | $\langle \xi \rangle_{K^*}^\parallel$ | $\langle \xi^2 \rangle_{K^*}^\parallel$ | $\langle \xi \rangle_{K^*}^\perp$ | $\langle \xi^2 \rangle_{K^*}^\perp$ |
|-------------------|--|------------------------------------|---------------------------------------|---|-----------------------------------|-------------------------------------|
| this work         | 0.259                                  | 0.236                              | 0.023                                 | 0.220                                   | 0.033                             | 0.210                               |
| lattice(21)' [13] | -                                      | -                                  | 0.003(4)                              | 0.205(3)                                | 0.044(4)                          | 0.262(4)                            |
| lattice(17)' [10] | 0.245(9)                               | 0.235(8)                           | -                                     | -                                       | -                                 | -                                   |
| lattice(10) [8]   | 0.27(2)                                | -                                  | 0.043(3)                              | 0.25(2)                                 | -                                 | -                                   |
| DSE(22) [40]      | 0.263                                  | 0.250                              | 0.018                                 | 0.272                                   | 0.056                             | 0.298                               |
| DSE(21) [39]      | 0.224(12)                              | 0.240(4)                           | -                                     | -                                       | -                                 | -                                   |
| DSE(14) [31]      | 0.23                                   | 0.25                               | -                                     | -                                       | -                                 | -                                   |
| sum rule' [18]    | 0.234(17)                              | 0.238(17)                          | 0.0012(12)                            | 0.227(21)                               | 0.0018(18)                        | 0.227(21)                           |

**Table 3.** Compare the first and second Mellin moments of  $\rho$  and  $K^*$  meson with the results of other approaches. The symbol ' denotes results derived from the Gegenbauer moments reported in the main text or supplementary materials of their paper, following eq. (3.6). Where  $\langle \xi^m \rangle$  is defined in eq. (3.2).

the predictions are generally consistent across different approaches. In contrast, the results for the  $K^*$  meson show slight variations. Specifically, the second moments of the  $K^*$  meson in our study are lower than those from DSE(22) [40] but closer to predictions from QCD sum rules [18]. Nevertheless, the differences between transverse and longitudinal moments reported by various approaches are small [18, 40], except for ref. [13], which shows a significant splitting. Given the limited studies on  $K^*$  mesons, further comparisons using diverse methods are essential.

Different from  $u\bar{d}$ ,  $u\bar{s}$ , ..., heavy-light systems, such as  $u\bar{c}$ ,  $u\bar{b}$ ,  $c\bar{s}$  exhibit higher flavor asymmetry, providing richer insight into the internal structure and dynamics of QCD bound states. As a result, their DAs may show larger asymmetry, which is reflected in the first moment. In table 4 and more intuitive figure 4, we compare the  $\langle \xi \rangle$  of heavy-light mesons obtained in this work with previous DSE results, alongside predictions from other models. The results indicate qualitative consistency across different approaches, higher flavor asymmetry corresponds to a larger  $\langle \xi \rangle$ . Besides, we note that the effect of valence quark spin-flip is smaller than that of flavor asymmetry, which is consistent with the results of LFQM(19) [29]. For flavor-asymmetric systems with identical valence quark structures, our results show  $\langle \xi \rangle_{0^-} \leq \langle \xi \rangle_{1^-}^\parallel \leq \langle \xi \rangle_{1^-}^\perp$ , suggesting heavier quarks in vector mesons carry more light-front momentum than in pseudo-scalar mesons. The full results of pseudo-scalar/vector meson's first eight moments can be found in the appendix A. In the next subsection, we will reconstruct their DAs using these data and provide further discussion.

|                    | this work | DSE(19) [37] | DSE(20) [38] | DSE(22) [40] | LFQM(10) [28] | LFQM(19) [29] | AM [25]   |
|--------------------|-----------|--------------|--------------|--------------|---------------|---------------|-----------|
| $K$                | 0.018     | -            | 0.124(13)    | -            | -             | -             | -         |
| $K^{*\parallel}$   | 0.023     | -            | -            | 0.018        | -             | -             | -         |
| $K^{*\perp}$       | 0.033     | -            | -            | 0.056        | -             | -             | -         |
| $D$                | 0.288     | 0.36(2)      | 0.266(17)    | -            | 0.288,0.251   | 0.325         | 0.365(13) |
| $D^{*\parallel}$   | 0.331     | -            | -            | 0.388        | -             | 0.356         | -         |
| $D^{*\perp}$       | 0.356     | -            | -            | 0.484        | -             | 0.351         | -         |
| $D_s$              | 0.271     | 0.34(2)      | 0.156(18)    | -            | 0.213,0.207   | 0.311         | 0.335(14) |
| $D_s^{*\parallel}$ | 0.308     | -            | -            | 0.254        | -             | 0.323         | -         |
| $D_s^{*\perp}$     | 0.330     | -            | -            | 0.310        | -             | 0.321         | -         |
| $B$                | 0.608     | 0.62(2)      | 0.666(10)    | -            | 0.617,0.531   | 0.665         | 0.616(20) |
| $B^{*\parallel}$   | 0.656     | -            | -            | -            | -             | 0.672         | -         |
| $B^{*\perp}$       | 0.671     | -            | -            | -            | -             | 0.672         | -         |
| $B_s$              | 0.594     | 0.60(2)      | 0.642(6)     | -            | 0.549,0.486   | 0.651         | 0.589(24) |
| $B_s^{*\parallel}$ | 0.629     | -            | -            | -            | -             | 0.652         | -         |
| $B_s^{*\perp}$     | 0.653     | -            | -            | -            | -             | 0.653         | -         |
| $B_c$              | 0.374     | 0.42(2)      | 0.464(4)     | -            | 0.536,0.368   | -             | 0.413(35) |
| $B_c^{*\parallel}$ | 0.405     | -            | -            | -            | -             | -             | -         |
| $B_c^{*\perp}$     | 0.416     | -            | -            | -            | -             | -             | -         |

**Table 4.** Compare the first Mellin moments  $\langle \xi \rangle$  of flavor-asymmetric mesons with the results of other DSE and some effective models, where  $\langle \xi^m \rangle$  is defined in eq. (3.2). A more intuitive illustration is shown in figure 4.

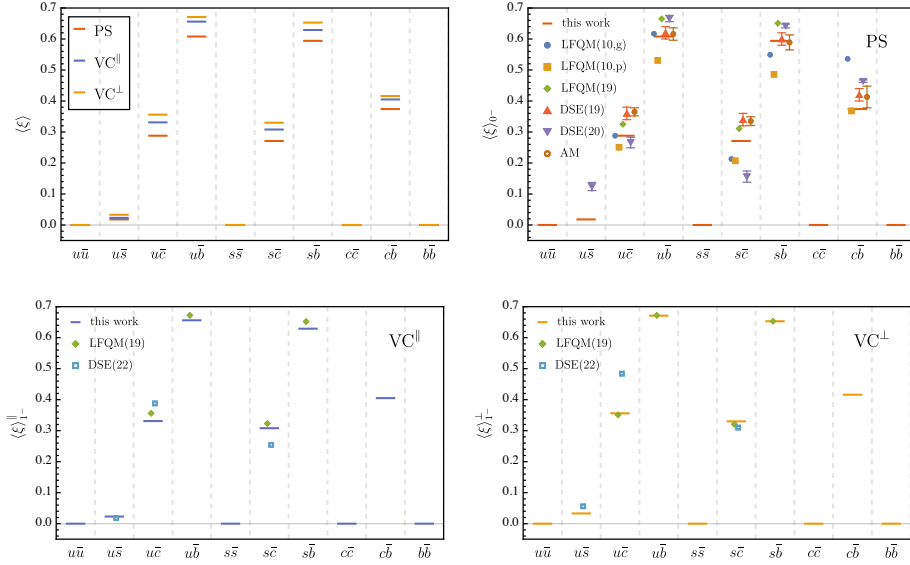


**Figure 4.** The first Mellin moments  $\langle \xi \rangle$  of pseudo-scalar/vector mesons, where  $\langle \xi^m \rangle$  is defined in eq. (3.2). Upper left panel shows the results of this work and other panels are comparison. We work in the isospin-symmetric limit  $u = d$ , and more details can be found in table 4.

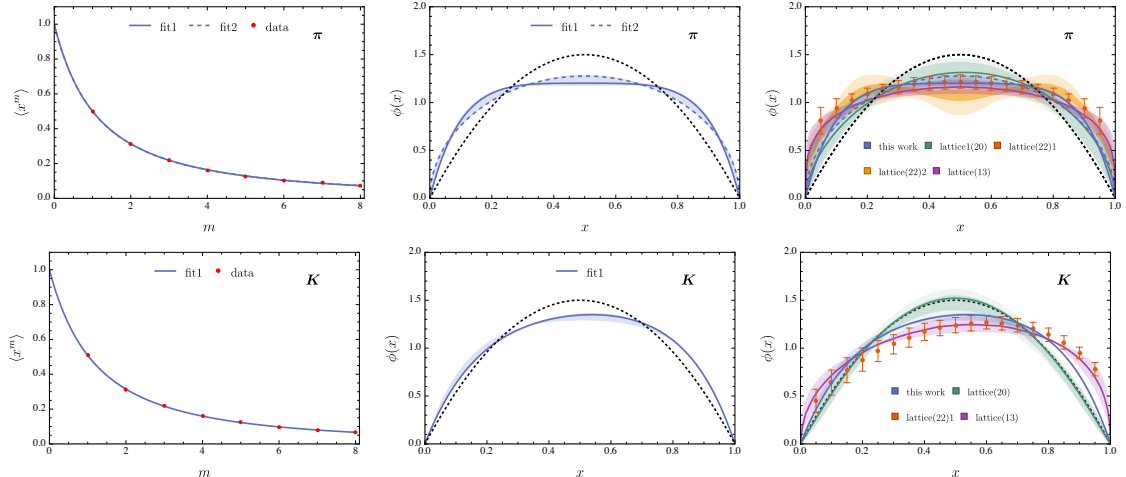


**Figure 5.** Reconstruct the DAs of the pion and kaon and compare them with recent lattice results: lattice(13) [9], lattice(20) [12], lattice(22)1 [7] and lattice(22)2 [14].

### 3.2 Distribution amplitudes

Due to the limited number of calculable moments, current reconstructions of DAs based on moments primarily rely on fitting a prior model. For heavy-light and heavy mesons, one widely used ansatz is [25, 34, 37, 38, 40]

$$\phi(x; \alpha, \beta) = \mathcal{N}(\alpha, \beta) 4x(1-x)e^{4\alpha x(1-x) + \beta(2x-1)}, \quad (3.7)$$

where  $\alpha$  and  $\beta$  are fitting parameters and  $\mathcal{N}(\alpha, \beta)$  is the normalization constant, which ensures that  $\int_0^1 dx \phi(x) = 1$ . It is worth noting that although  $\mathcal{N}(\alpha, \beta)$  has an analytical form based on special functions, its value should be more reliably determined through numerical integration due to the potential impact of floating-point errors <sup>1</sup>.

To ensure consistency in the analysis, eq. (3.7) is uniformly applied as the fitting model (fit1) for reconstructing the meson DAs in this work. The reliability of this ansatz is evaluated by extracting 3 out of 8 moments as fitting data, which generates  $C_3^8 = 56$  subsets for establishing the error band. In particular, for the  $\pi$  and  $\rho$  mesons, another commonly used model, eq. (3.8), is also employed for comparison (fit2) [30, 31]:

$$\phi(x; a) = \mathcal{N}(a)x^a(1-x)^a. \quad (3.8)$$

The upper panels of figure 5 present the fitting process for the pion's DAs. Both models yield satisfactory fits, though slight fluctuations appear in fit1 around  $x \sim 0.5$ . Similarly, the lower panels illustrate the kaon's DAs, with  $\phi(x)$  noticeably skewed due to SU(3) flavor symmetry breaking. The right panels of figure 5 highlight the consistency between our results and lattice QCD data for both the pion and kaon. Additionally, comparisons of heavy-light pseudo-scalar meson DAs with existing DSE [37, 38, 41] and lattice studies [15]

<sup>1</sup>For example, when  $\alpha = 0.2$ ,  $\beta = 5$ , the analytical form of the normalization constant is 0.2179 in double precision, but 0.1895 in quadruple precision. In contrast, the normalization constant obtained through numerical integration consistently remains at 0.1895 in both double and quadruple precision.

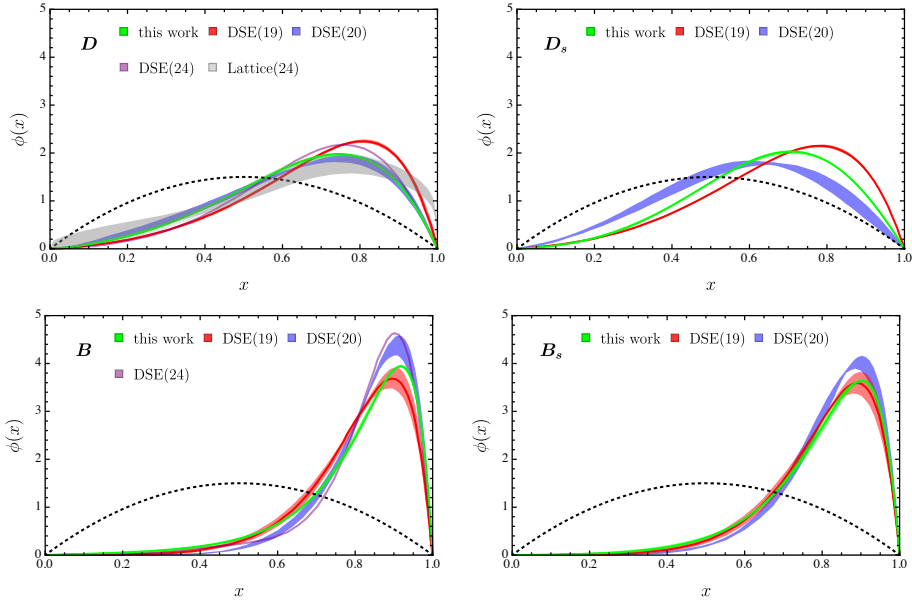


**Figure 6.** Compare the DAs of heavy-light pseudo-scalar meson with the results of DSE(19) [37], DSE(20) [38], DSE(24) [41] and lattice(24) [15]. The black dotted lines mark the asymptotic limit.

reveal qualitative agreement (see figure 6). The final reconstructed DAs of pseudo-scalar and vector meson are shown in figure 7, while details of the complete fitting process are provided in the appendix A.

According to ref. [110], at tree level, and in leading order of the expansion in the relative velocities, the quark and the antiquark in the non-relativistic (NR) wave function simply share the momentum of the meson according to their masses, and DAs may have the following form:

$$\phi^{\text{NR}}(x) \simeq \delta(x - x'), \quad x' = m_1/(m_1 + m_2), \quad (3.9)$$

where  $x$  denotes the light-cone momentum fraction of the quark, and  $m_{1,2}$  are the masses of the (anti-)quark, respectively. Hence, it is reasonable to conjecture that for ground-state pseudo-scalar and vector flavor-symmetric  $q\bar{q}$  mesons,  $\phi(x)$  broadens around  $x = 1/2$  as the current-quark mass decreases, due to the increasing dressed effect. This hypothesis has been consistently validated by previous DSE studies [34, 38, 40], despite variations in the specific widths. Our results further support this perspective (see figure 7, upper panels). Compared with the asymptotic limit  $\phi^{\text{asy}}(x)$ , the DAs of the  $\pi$  and  $\rho$  mesons appear broader, whereas those of the  $\phi$  meson are slightly narrower, with  $\phi_{\phi}^{\parallel}(x, \mu) \approx \phi_{\phi}^{\perp}(x, \mu)$ . Notably, a similar conclusion for the  $\phi$  meson has been reported in DSE(22), although it is sensitive to the current-quark mass [40].

For heavy-light systems, we observe that their DAs gradually narrow and become increasingly skewed to one side as flavor asymmetry increases (see figure 7). This can be interpreted as the heavier quark carrying more light-front momentum in this system. To better reflect the variation of DAs with the current-quark mass and flavor asymmetry,

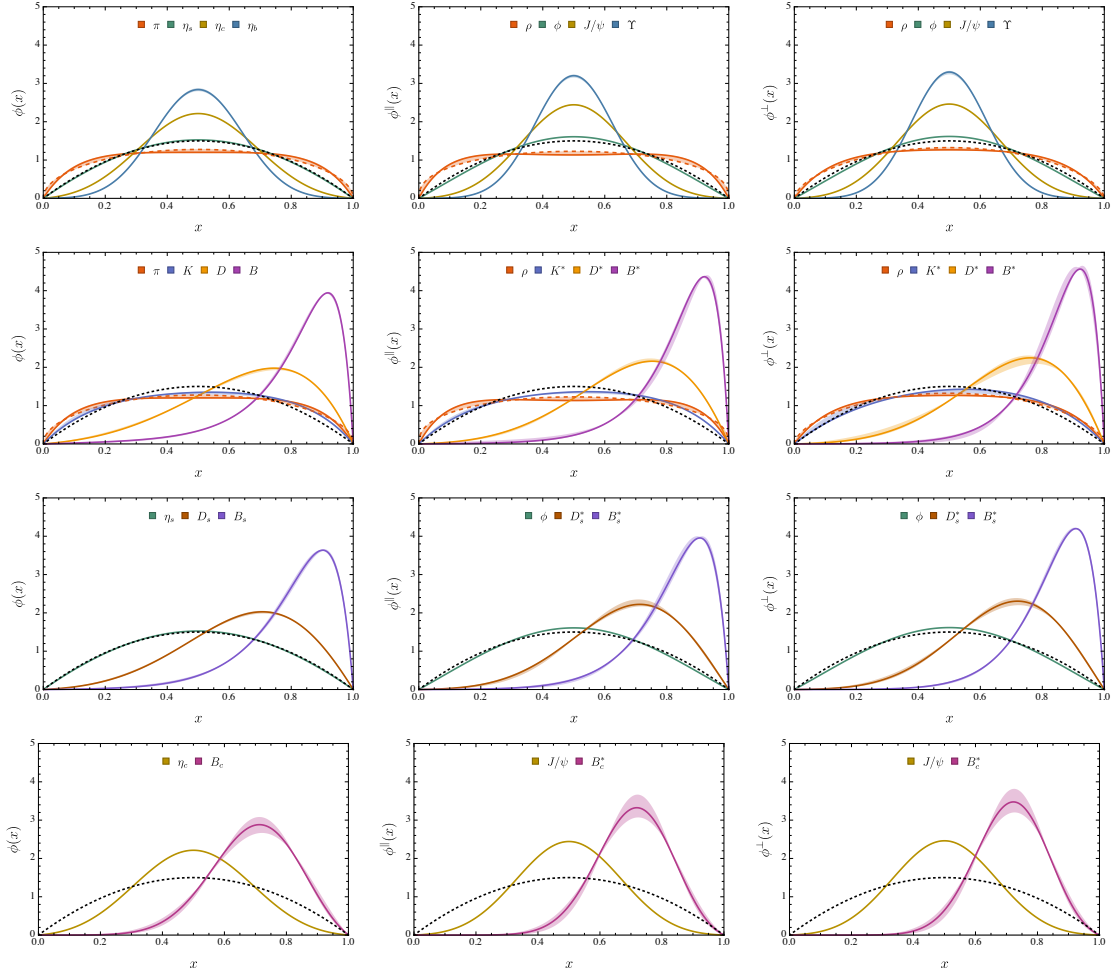


**Figure 7.** The full results of pseudo-scalar and vector meson DAs. The black dotted lines mark the asymptotic limit.

we extract two quantities: the position of the maximum,  $x_0$ , and the full width at half maximum (FWHM),  $\Delta_x$  (see table 5 and more intuitive figure 8).

As mentioned below eq. (2.5), the Euclidean constituent quark mass  $M_E$  serves as a realistic estimate of the quark's active quasi-particle mass. Inspired by eq. (3.9), we define

$$x_{M_E} = M_E^f / (M_E^f + M_E^g), \quad (3.10)$$

where  $f$  and  $g$  represent the heavier and lighter quark flavors in the meson, respectively. This definition allows us to compare  $x_{M_E}$  with the position of the DA's maximum,  $x_0$ . Interestingly, our results show that  $x_0$  and  $x_{M_E}$  nearly coincide, except for a deviation of approximately 7% in the  $c\bar{b}$  system (see, figure 8, left panel). Considering the larger error bands of reconstructed DAs near  $x_0$  for  $B_c^{(*)}$  meson (see the last row of figure 7), this suggests that  $\phi(x)$  for ground-state pseudo-scalar and vector mesons may be approximated as a finite-width expansion of the  $\delta$ -function centered at  $x_{M_E}$ . The right panel of figure 8 shows that the width  $\Delta_x$  of  $u\bar{q}$ ,  $s\bar{q}$ ,  $c\bar{q}$  systems generally decrease with increasing current



| Meson              |            | $x_{M_E}$ | $x_0$                     |                           |                           | $\Delta_x$                |                           |                           |
|--------------------|------------|-----------|---------------------------|---------------------------|---------------------------|---------------------------|---------------------------|---------------------------|
|                    |            |           | PS                        | VC <sup>  </sup>          | VC <sup>⊥</sup>           | PS                        | VC <sup>  </sup>          | VC <sup>⊥</sup>           |
| $\pi, \rho$        | $u\bar{u}$ | 0.500     | $0.500^{+0.000}_{-0.000}$ | $0.500^{+0.000}_{-0.000}$ | $0.500^{+0.000}_{-0.000}$ | $0.863^{+0.010}_{-0.011}$ | $0.903^{+0.003}_{-0.004}$ | $0.826^{+0.005}_{-0.005}$ |
| $K, K^*$           | $u\bar{s}$ | 0.536     | $0.538^{+0.004}_{-0.029}$ | $0.546^{+0.002}_{-0.016}$ | $0.552^{+0.002}_{-0.033}$ | $0.798^{+0.034}_{-0.010}$ | $0.790^{+0.028}_{-0.006}$ | $0.751^{+0.061}_{-0.009}$ |
| $D, D^*$           | $u\bar{c}$ | 0.759     | $0.745^{+0.008}_{-0.003}$ | $0.753^{+0.004}_{-0.006}$ | $0.761^{+0.016}_{-0.007}$ | $0.500^{+0.014}_{-0.003}$ | $0.455^{+0.004}_{-0.015}$ | $0.436^{+0.031}_{-0.011}$ |
| $B, B^*$           | $u\bar{b}$ | 0.910     | $0.918^{+0.002}_{-0.005}$ | $0.921^{+0.009}_{-0.004}$ | $0.922^{+0.007}_{-0.014}$ | $0.216^{+0.007}_{-0.004}$ | $0.201^{+0.006}_{-0.015}$ | $0.195^{+0.012}_{-0.010}$ |
| $\eta_s, \phi$     | $s\bar{s}$ | 0.500     | $0.500^{+0.000}_{-0.000}$ | $0.500^{+0.000}_{-0.000}$ | $0.500^{+0.000}_{-0.000}$ | $0.692^{+0.002}_{-0.001}$ | $0.647^{+0.005}_{-0.002}$ | $0.643^{+0.003}_{-0.002}$ |
| $D_s, D_s^*$       | $s\bar{c}$ | 0.731     | $0.707^{+0.003}_{-0.003}$ | $0.713^{+0.006}_{-0.004}$ | $0.720^{+0.004}_{-0.004}$ | $0.489^{+0.012}_{-0.007}$ | $0.443^{+0.012}_{-0.026}$ | $0.426^{+0.021}_{-0.016}$ |
| $B_s, B_s^*$       | $s\bar{b}$ | 0.897     | $0.902^{+0.005}_{-0.006}$ | $0.907^{+0.007}_{-0.009}$ | $0.908^{+0.004}_{-0.005}$ | $0.246^{+0.005}_{-0.005}$ | $0.229^{+0.006}_{-0.008}$ | $0.218^{+0.003}_{-0.003}$ |
| $\eta_c, J/\psi$   | $c\bar{c}$ | 0.500     | $0.500^{+0.000}_{-0.000}$ | $0.500^{+0.000}_{-0.000}$ | $0.500^{+0.000}_{-0.000}$ | $0.436^{+0.002}_{-0.001}$ | $0.391^{+0.002}_{-0.002}$ | $0.388^{+0.003}_{-0.001}$ |
| $B_c, B_c^*$       | $c\bar{b}$ | 0.762     | $0.713^{+0.008}_{-0.002}$ | $0.719^{+0.004}_{-0.002}$ | $0.722^{+0.004}_{-0.002}$ | $0.335^{+0.030}_{-0.023}$ | $0.288^{+0.026}_{-0.028}$ | $0.275^{+0.026}_{-0.026}$ |
| $\eta_b, \Upsilon$ | $b\bar{b}$ | 0.500     | $0.500^{+0.000}_{-0.000}$ | $0.500^{+0.000}_{-0.000}$ | $0.500^{+0.000}_{-0.000}$ | $0.334^{+0.005}_{-0.004}$ | $0.295^{+0.005}_{-0.003}$ | $0.286^{+0.005}_{-0.003}$ |

**Table 5.** This table presents an analysis of meson DAs (see figure 7), and we work in the isospin-symmetric limit  $u = d$ . Here,  $x_0$  denotes the position of the maximum,  $\Delta_x$  represents the FWHM, and  $x_{M_E}$  is defined in eq. (3.10). The reconstruction of DAs predominantly employs fit1, except for  $\pi$  and  $\rho$ , which utilize fit2 due to fluctuations around  $x \sim 0.5$  observed under fit1. If  $\Delta_x$  is redefined as the full width at  $\phi(x)/2|_{x=0.5}$  for fit1, the results are  $\Delta_x^\pi = 0.875^{+0.013}_{-0.013}$ ,  $\Delta_x^{\rho^||} = 0.902^{+0.007}_{-0.007}$ ,  $\Delta_x^{\rho^\perp} = 0.843^{+0.009}_{-0.009}$ , which are approximately consistent with those obtained using fit2. An intuitive comparison is illustrated in figure 8.

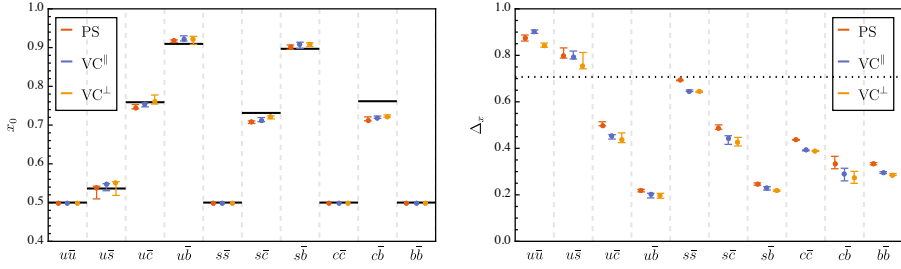


**Figure 8.** This figure illustrates an analysis of meson DAs (see figure 7). The left panel depicts the position of the maximum  $x_0$ , with black lines indicating  $x_{M_E}$  (see eq. (3.10)). The right panel shows the full width at half maximum (FWHM)  $\Delta_x$ , where the black dotted line represents the FWHM of the asymptotic limit ( $\sim 0.707$ ). More details can be found in table 5.

mass of  $q = u, s, c, b$  quark. For all systems except  $u\bar{u}$  and  $u\bar{s}$ ,  $\Delta_x$  are below the asymptotic limit ( $\sim 0.707$ ).

When the valence quark structure of flavor-asymmetric systems is identical, we observe  $x_0^{0^-} \lesssim x_0^{1^-,||} \lesssim x_0^{1^-,\perp}$  (see figure 8, left panel), consistent with the conjecture based on the first moment analysis in the previous subsection. However, the effect of valence quark spin-flip is smaller than that of flavor asymmetry, as reported in the studies of the electromagnetic form factor [60]. We note that the DAs of  $K^*$ ,  $D^*$ , and  $D_s^*$  mesons have been investigated in ref. [40] with a comparable approach, revealing  $x_0^{1^-,||} \lesssim x_0^{1^-,\perp}$ . Our results support this conclusion, although the effective heavy-light kernel applied is different. Additionally, it is found that  $\Delta_x^{0^-} \gtrsim \Delta_x^{1^-,||} \gtrsim \Delta_x^{1^-,\perp}$  for flavor-asymmetric mesons (see, figure 8, right panel). However, this relation should be approached with caution due to the larger error bars and further studies are required.

## 4 Summary and Perspectives

In this work, we systematically investigate the leading-twist DAs of ground-state heavy-light pseudo-scalar and vector mesons. Notably, the results of  $B^*$ ,  $B_s^*$ , and  $B_c^*$  mesons are reported for the first time within the DSEs/BSEs framework. We also propose a novel numerical method for calculating Mellin moments. The key step involves iterating the BSE in two-dimensional Chebyshev tensor grid to obtain a continuous BS wave function, followed by a modern multi-dimensional adaptive integration algorithm to efficiently evaluate highly oscillatory integrals, eliminating the need for extrapolation or fitting in previous similar studies.

Based on it, we calculate the first eight Mellin moments of pseudo-scalar and vector mesons and reconstruct their DAs. The results show that as the current mass of the  $q = u, s, c, b$  quark increases, the DAs of flavor-symmetric  $q\bar{q}$  mesons gradually narrow, consistent with previous DSE studies. For flavor-asymmetric  $u\bar{q}$ ,  $s\bar{q}$ , and  $c\bar{q}$  mesons, the DAs not only narrow but also exhibit skewness, with the maximum located near  $M_E^f/(M_E^f + M_E^g)$ , where  $M_E$  denotes the Euclidean constituent quark mass and  $f/g$  indicate the heavier/lighter quark flavors, respectively. For all systems except  $u\bar{u}$  and  $u\bar{s}$ , the full width at half maximum (FWHM)  $\Delta_x$  is below the asymptotic limit ( $\sim 0.707$ ).

Furthermore, the comparison of these DAs reveals that the effect of valence quark spin-flip is smaller than that of flavor asymmetry. For flavor-asymmetric systems with identical valence quark structures, the first Mellin moments follow  $\langle \xi \rangle_{0^-} < \langle \xi \rangle_{1^-}^{\parallel} < \langle \xi \rangle_{1^-}^{\perp}$ , where  $\xi = 2x - 1$  and  $x$  represents the momentum fraction carried by the heavier quark. The reconstructed DAs show maxima positions satisfying  $x_0^{0^-} \lesssim x_0^{1^-,\parallel} \lesssim x_0^{1^-,\perp}$ , indicating heavier quarks in vector mesons carry more light-front momentum than in pseudo-scalar mesons. Additionally, the FWHM of flavor-asymmetric mesons imply  $\Delta_x^{0^-} \gtrsim \Delta_x^{1^-,\parallel} \gtrsim \Delta_x^{1^-,\perp}$ , however, this relation should be approached with caution and further studies are required.

Our predictions can be compared with both experimental and theoretical outcomes in the future, and the results for light mesons such as  $\pi$ ,  $K$ , and  $\rho$  align well with recent lattice data. The numerical method proposed for calculating Mellin moments is readily applicable to other mesons, including excited states. It is worth noting that, in this work we employ an effective kernel within the RL framework. Future comparisons using other effective kernels are important, and the results could be improved by more elaborate beyond-RL kernels. We expect that it will be useful for the understanding of the internal structure and dynamics of QCD's bound states.

### A Fitting DAs based on Mellin moments

The first eight Mellin moments of pseudo-scalar and vector mesons are listed in table 6, 7, 8, and the fittings are shown in figure 9, 10, 11.

|          | $\langle x \rangle$ | $\langle x^2 \rangle$ | $\langle x^3 \rangle$ | $\langle x^4 \rangle$ | $\langle x^5 \rangle$ | $\langle x^6 \rangle$ | $\langle x^7 \rangle$ | $\langle x^8 \rangle$ | $\alpha$                   | $\beta$                   |
|----------|---------------------|-----------------------|-----------------------|-----------------------|-----------------------|-----------------------|-----------------------|-----------------------|----------------------------|---------------------------|
| $\pi$    | 0.500               | 0.311                 | 0.217                 | 0.163                 | 0.128                 | 0.105                 | 0.088                 | 0.075                 | $-0.986^{+0.094}_{-0.101}$ | 0                         |
| $K$      | 0.509               | 0.315                 | 0.216                 | 0.159                 | 0.123                 | 0.098                 | 0.081                 | 0.067                 | $-0.510^{+0.058}_{-0.189}$ | $0.076^{+0.006}_{-0.064}$ |
| $\eta_s$ | 0.500               | 0.299                 | 0.199                 | 0.141                 | 0.105                 | 0.082                 | 0.065                 | 0.053                 | $0.086^{+0.005}_{-0.011}$  | 0                         |
| $D$      | 0.644               | 0.452                 | 0.336                 | 0.260                 | 0.207                 | 0.169                 | 0.142                 | 0.119                 | $0.382^{+0.066}_{-0.215}$  | $1.666^{+0.030}_{-0.136}$ |
| $D_s$    | 0.635               | 0.440                 | 0.321                 | 0.243                 | 0.191                 | 0.154                 | 0.127                 | 0.105                 | $0.902^{+0.114}_{-0.167}$  | $1.750^{+0.060}_{-0.106}$ |
| $\eta_c$ | 0.500               | 0.279                 | 0.169                 | 0.109                 | 0.074                 | 0.052                 | 0.038                 | 0.028                 | $2.530^{+0.026}_{-0.030}$  | 0                         |
| $B$      | 0.804               | 0.670                 | 0.570                 | 0.495                 | 0.433                 | 0.382                 | 0.342                 | 0.307                 | $-1.419^{+0.476}_{-0.176}$ | $3.171^{+0.478}_{-0.181}$ |
| $B_s$    | 0.797               | 0.657                 | 0.553                 | 0.473                 | 0.410                 | 0.358                 | 0.318                 | 0.284                 | $-0.464^{+0.503}_{-0.475}$ | $3.780^{+0.515}_{-0.498}$ |
| $B_c$    | 0.687               | 0.494                 | 0.366                 | 0.278                 | 0.214                 | 0.169                 | 0.135                 | 0.110                 | $4.161^{+0.986}_{-1.093}$  | $4.586^{+0.833}_{-0.771}$ |
| $\eta_b$ | 0.500               | 0.269                 | 0.153                 | 0.092                 | 0.058                 | 0.038                 | 0.025                 | 0.018                 | $5.167^{+0.173}_{-0.192}$  | 0                         |

**Table 6.** First eight order Mellin moments  $\langle x^m \rangle$  of pseudo-scalar mesons, where  $\alpha$ ,  $\beta$  are fit1's parameters, and the fit2's parameter  $a_\pi$  is  $0.506^{+0.028}_{-0.025}$ .

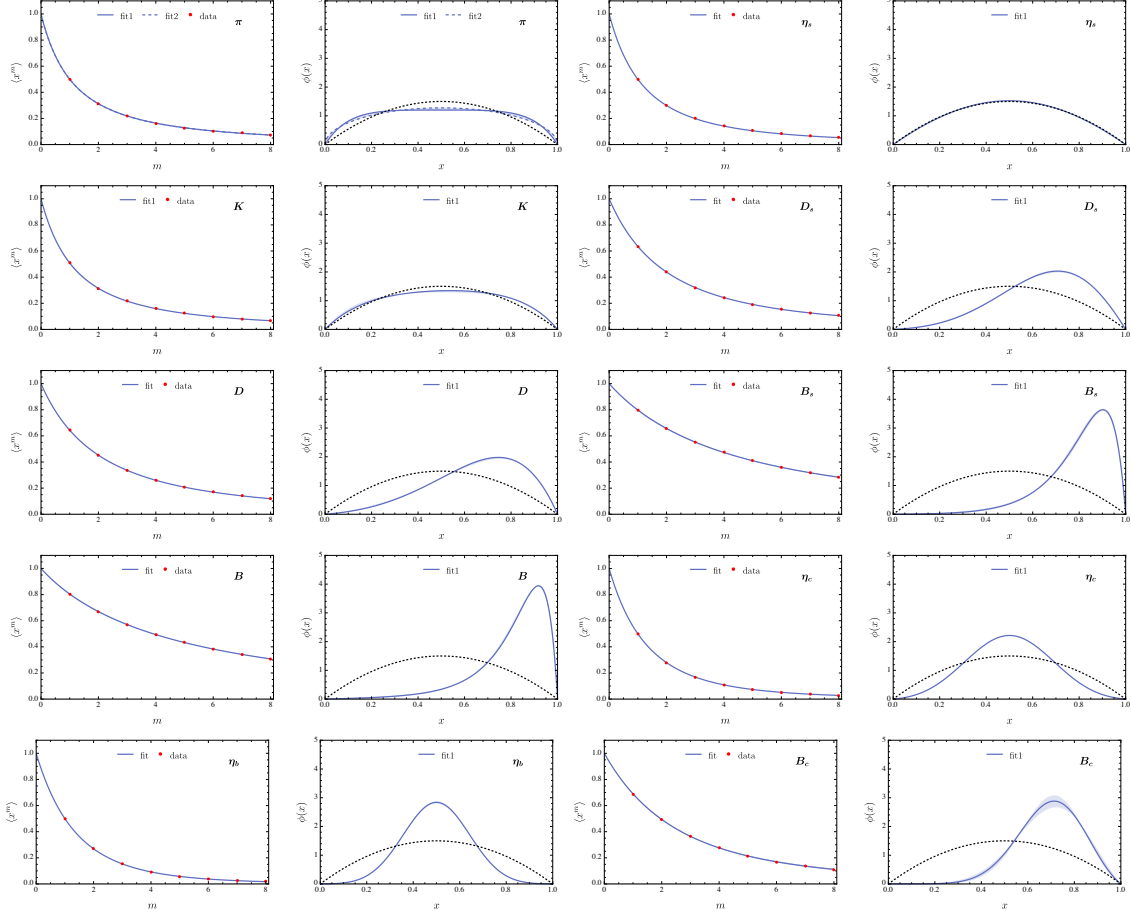


**Figure 9.** Fitting DAs based on Mellin moments (see table 6). The black dotted lines mark the asymptotic limit.

|            | $\langle x \rangle^{\parallel}$ | $\langle x^2 \rangle^{\parallel}$ | $\langle x^3 \rangle^{\parallel}$ | $\langle x^4 \rangle^{\parallel}$ | $\langle x^5 \rangle^{\parallel}$ | $\langle x^6 \rangle^{\parallel}$ | $\langle x^7 \rangle^{\parallel}$ | $\langle x^8 \rangle^{\parallel}$ | $\alpha$                   | $\beta$                   |
|------------|---------------------------------|-----------------------------------|-----------------------------------|-----------------------------------|-----------------------------------|-----------------------------------|-----------------------------------|-----------------------------------|----------------------------|---------------------------|
| $\rho$     | 0.500                           | 0.315                             | 0.223                             | 0.169                             | 0.134                             | 0.110                             | 0.093                             | 0.080                             | $-1.212^{+0.066}_{-0.069}$ | 0                         |
| $K^*$      | 0.512                           | 0.317                             | 0.218                             | 0.160                             | 0.123                             | 0.099                             | 0.080                             | 0.067                             | $-0.470^{+0.030}_{-0.152}$ | $0.100^{+0.006}_{-0.053}$ |
| $\phi$     | 0.500                           | 0.296                             | 0.194                             | 0.136                             | 0.100                             | 0.077                             | 0.062                             | 0.049                             | $0.363^{+0.015}_{-0.030}$  | 0                         |
| $D^*$      | 0.666                           | 0.478                             | 0.358                             | 0.279                             | 0.223                             | 0.183                             | 0.151                             | 0.128                             | $0.787^{+0.296}_{-0.102}$  | $2.154^{+0.224}_{-0.064}$ |
| $D_s^*$    | 0.654                           | 0.460                             | 0.338                             | 0.258                             | 0.202                             | 0.162                             | 0.132                             | 0.109                             | $1.474^{+0.513}_{-0.244}$  | $2.297^{+0.375}_{-0.130}$ |
| $J/\psi$   | 0.500                           | 0.275                             | 0.163                             | 0.102                             | 0.067                             | 0.045                             | 0.032                             | 0.023                             | $3.439^{+0.053}_{-0.037}$  | 0                         |
| $B^*$      | 0.828                           | 0.702                             | 0.605                             | 0.527                             | 0.465                             | 0.413                             | 0.372                             | 0.338                             | $-0.983^{+0.512}_{-1.248}$ | $4.145^{+0.550}_{-1.339}$ |
| $B_s^*$    | 0.814                           | 0.680                             | 0.579                             | 0.502                             | 0.437                             | 0.385                             | 0.341                             | 0.305                             | $-0.179^{+1.061}_{-0.676}$ | $4.513^{+1.226}_{-0.673}$ |
| $B_c^*$    | 0.703                           | 0.510                             | 0.380                             | 0.288                             | 0.222                             | 0.174                             | 0.138                             | 0.110                             | $6.312^{+1.924}_{-1.398}$  | $6.610^{+1.775}_{-1.106}$ |
| $\Upsilon$ | 0.500                           | 0.265                             | 0.147                             | 0.086                             | 0.052                             | 0.033                             | 0.021                             | 0.014                             | $6.930^{+0.161}_{-0.250}$  | 0                         |

**Table 7.** First eight order Mellin moments  $\langle x^m \rangle^{\parallel}$  of vector meson (longitudinally), where  $\alpha$ ,  $\beta$  are fit1's parameters, and the fit2's parameter  $a_{\rho^{\parallel}}$  is  $0.409^{+0.009}_{-0.007}$ .

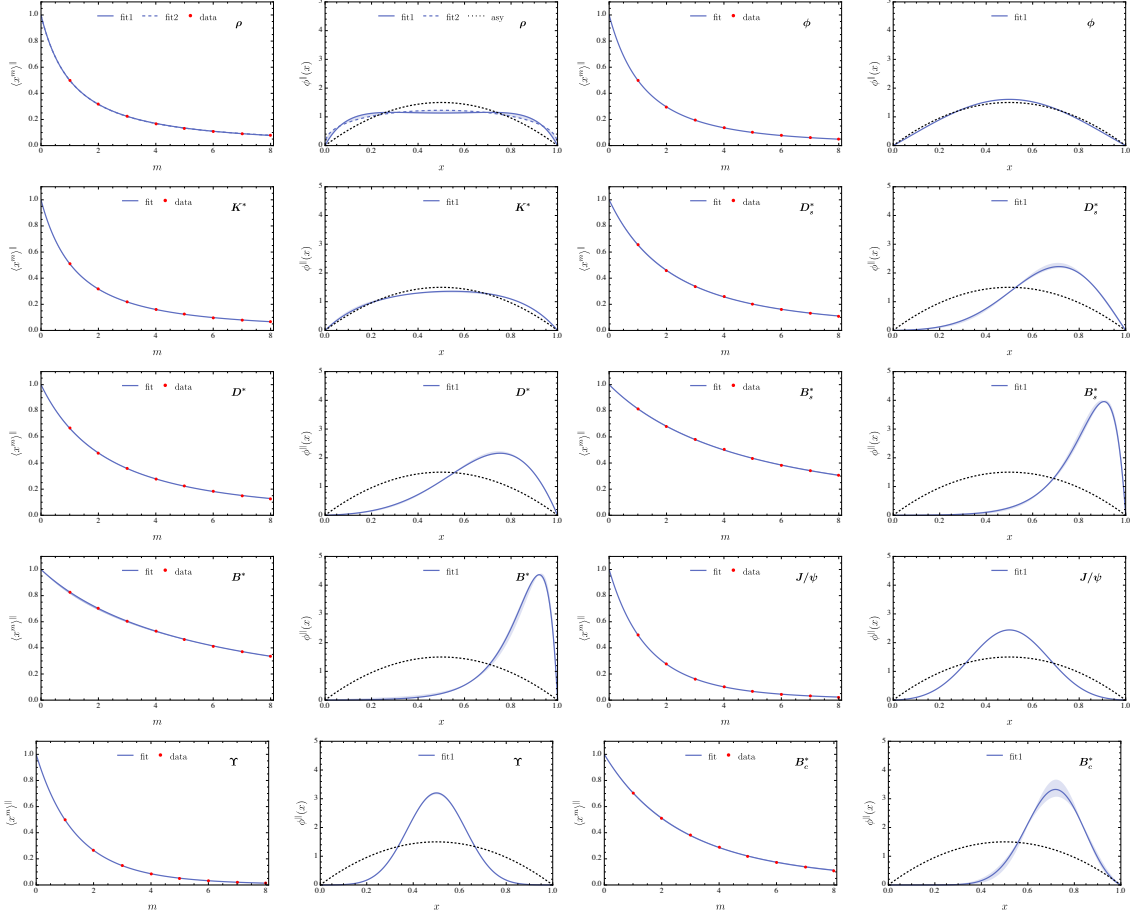


**Figure 10.** Fitting DAs of vector meson (longitudinally) based on Mellin moments (see table 7). The black dotted lines mark the asymptotic limit.

|            | $\langle x \rangle^\perp$ | $\langle x^2 \rangle^\perp$ | $\langle x^3 \rangle^\perp$ | $\langle x^4 \rangle^\perp$ | $\langle x^5 \rangle^\perp$ | $\langle x^6 \rangle^\perp$ | $\langle x^7 \rangle^\perp$ | $\langle x^8 \rangle^\perp$ | $\alpha$                   | $\beta$                   |
|------------|---------------------------|-----------------------------|-----------------------------|-----------------------------|-----------------------------|-----------------------------|-----------------------------|-----------------------------|----------------------------|---------------------------|
| $\rho$     | 0.500                     | 0.309                       | 0.214                       | 0.158                       | 0.123                       | 0.099                       | 0.082                       | 0.070                       | $-0.772^{+0.054}_{-0.061}$ | 0                         |
| $K^*$      | 0.517                     | 0.319                       | 0.219                       | 0.159                       | 0.123                       | 0.097                       | 0.079                       | 0.066                       | $-0.269^{+0.052}_{-0.313}$ | $0.153^{+0.006}_{-0.122}$ |
| $\phi$     | 0.500                     | 0.296                       | 0.194                       | 0.136                       | 0.100                       | 0.077                       | 0.061                       | 0.049                       | $0.389^{+0.013}_{-0.022}$  | 0                         |
| $D^*$      | 0.678                     | 0.491                       | 0.371                       | 0.290                       | 0.233                       | 0.190                       | 0.160                       | 0.135                       | $0.925^{+0.296}_{-0.649}$  | $2.405^{+0.209}_{-0.492}$ |
| $D_s^*$    | 0.665                     | 0.471                       | 0.349                       | 0.267                       | 0.209                       | 0.168                       | 0.138                       | 0.115                       | $1.680^{+0.352}_{-0.399}$  | $2.571^{+0.248}_{-0.308}$ |
| $J/\psi$   | 0.500                     | 0.275                       | 0.162                       | 0.101                       | 0.066                       | 0.045                       | 0.032                       | 0.023                       | $3.518^{+0.025}_{-0.063}$  | 0                         |
| $B^*$      | 0.835                     | 0.715                       | 0.619                       | 0.545                       | 0.484                       | 0.429                       | 0.384                       | 0.346                       | $-0.623^{+2.354}_{-0.958}$ | $4.818^{+2.925}_{-1.028}$ |
| $B_s^*$    | 0.827                     | 0.698                       | 0.598                       | 0.519                       | 0.456                       | 0.401                       | 0.358                       | 0.321                       | $0.318^{+0.735}_{-0.460}$  | $5.413^{+0.869}_{-0.508}$ |
| $B_c^*$    | 0.708                     | 0.517                       | 0.386                       | 0.293                       | 0.226                       | 0.177                       | 0.140                       | 0.112                       | $7.097^{+2.002}_{-1.563}$  | $7.420^{+1.877}_{-1.278}$ |
| $\Upsilon$ | 0.500                     | 0.264                       | 0.146                       | 0.084                       | 0.051                       | 0.032                       | 0.020                       | 0.014                       | $7.426^{+0.165}_{-0.314}$  | 0                         |

**Table 8.** First eight order Mellin moments  $\langle x^m \rangle^\perp$  of vector meson (transversely), where  $\alpha$ ,  $\beta$  are fit1's parameters, and the fit2's parameter  $a_{\rho^\perp}$  is  $0.605^{+0.013}_{-0.013}$ .

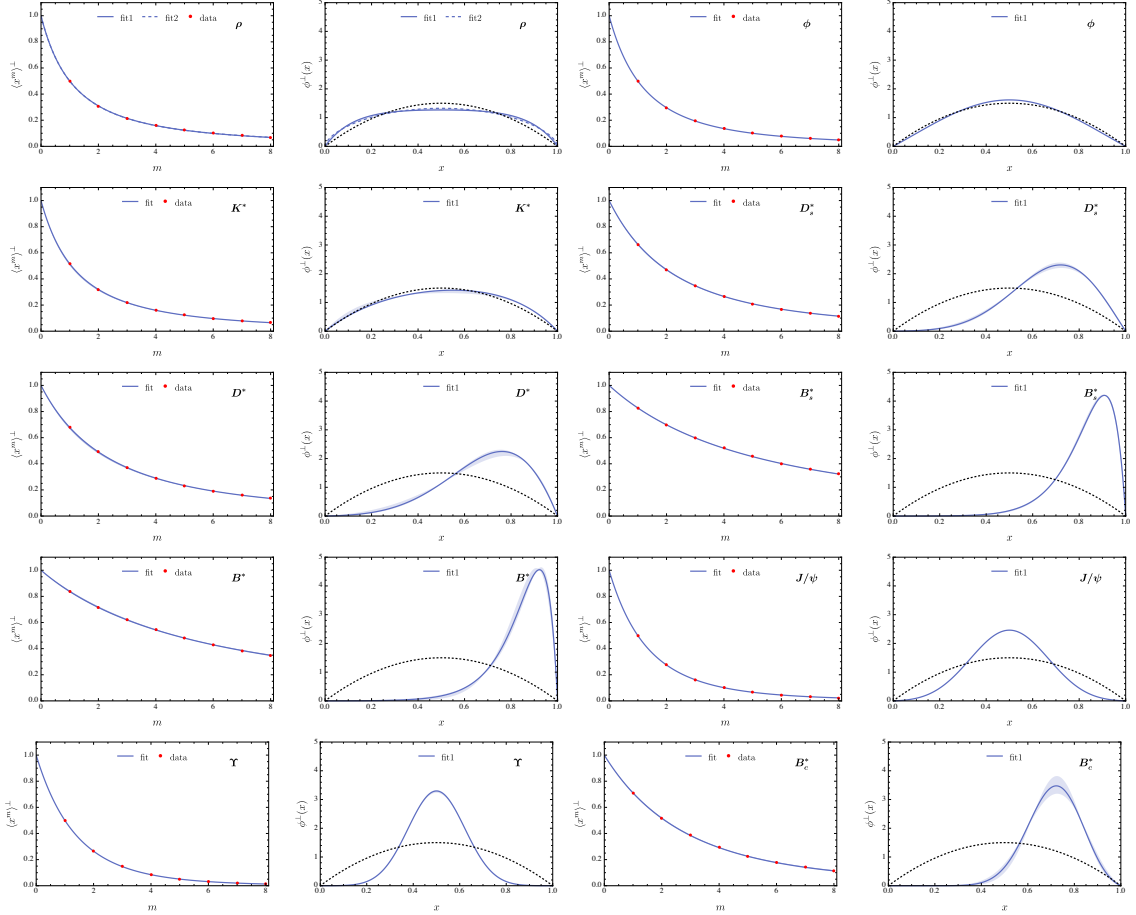


**Figure 11.** Fitting DAs of vector meson (transversely) based on Mellin moments (see table 8). The black dotted lines mark the asymptotic limit.

## Acknowledgments

This work has been partially funded by Ministerio Español de Ciencia e Innovación under grant Nos. PID2019-107844GB-C22 and PID2022-140440NB-C22; Junta de Andalucía under contract Nos. Operativo FEDER Andalucía 2014-2020 UHU-1264517, P18-FR-5057 and also PAIDI FQM-370. The authors acknowledge, too, the use of the computer facilities of C3UPO at the Universidad Pablo de Olavide, de Sevilla. We would like to thank Khépani Raya and José Rodríguez-Quintero for useful discussions.

## References

- [1] S.J. Brodsky, H.-C. Pauli and S.S. Pinsky, *Quantum chromodynamics and other field theories on the light cone*, *Phys. Rept.* **301** (1998) 299 [[hep-ph/9705477](#)].
- [2] P. Ball, *Theoretical update of pseudoscalar meson distribution amplitudes of higher twist: The Nonsinglet case*, *JHEP* **01** (1999) 010 [[hep-ph/9812375](#)].
- [3] A.P. Bakulev, S.V. Mikhailov and N.G. Stefanis, *What is this thing called pion distribution amplitude? From theory to data*, in *Light-Cone Workshop: Hadrons and Beyond (LC 03)*, 10, 2003 [[hep-ph/0310267](#)].
- [4] M. Beneke, G. Buchalla, M. Neubert and C.T. Sachrajda, *QCD factorization for  $B \rightarrow \pi$  decays: Strong phases and CP violation in the heavy quark limit*, *Phys. Rev. Lett.* **83** (1999) 1914 [[hep-ph/9905312](#)].
- [5] M. Beneke, G. Buchalla, M. Neubert and C.T. Sachrajda, *QCD factorization in  $B \rightarrow \pi K$ ,  $\pi\pi$  decays and extraction of Wolfenstein parameters*, *Nucl. Phys. B* **606** (2001) 245 [[hep-ph/0104110](#)].
- [6] G.P. Lepage and S.J. Brodsky, *Exclusive Processes in Quantum Chromodynamics: Evolution Equations for Hadronic Wave Functions and the Form-Factors of Mesons*, *Phys. Lett. B* **87** (1979) 359.
- [7] LATTICE PARTON collaboration, *Pion and Kaon Distribution Amplitudes from Lattice QCD*, *Phys. Rev. Lett.* **129** (2022) 132001 [[2201.09173](#)].
- [8] R. Arthur, P.A. Boyle, D. Brommel, M.A. Donnellan, J.M. Flynn, A. Juttner et al., *Lattice Results for Low Moments of Light Meson Distribution Amplitudes*, *Phys. Rev. D* **83** (2011) 074505 [[1011.5906](#)].
- [9] J. Segovia, L. Chang, I.C. Cloët, C.D. Roberts, S.M. Schmidt and H.-s. Zong, *Distribution amplitudes of light-quark mesons from lattice QCD*, *Phys. Lett. B* **731** (2014) 13 [[1311.1390](#)].
- [10] V.M. Braun et al., *The  $\rho$ -meson light-cone distribution amplitudes from lattice QCD*, *JHEP* **04** (2017) 082 [[1612.02955](#)].
- [11] RQCD collaboration, *Light-cone distribution amplitudes of pseudoscalar mesons from lattice QCD*, *JHEP* **08** (2019) 065 [[1903.08038](#)].
- [12] R. Zhang, C. Honkala, H.-W. Lin and J.-W. Chen, *Pion and kaon distribution amplitudes in the continuum limit*, *Phys. Rev. D* **102** (2020) 094519 [[2005.13955](#)].
- [13] LATTICE PARTON collaboration, *Distribution Amplitudes of  $K^*$  and  $\phi$  at the Physical Pion Mass from Lattice QCD*, *Phys. Rev. Lett.* **127** (2021) 062002 [[2011.09788](#)].

- [14] X. Gao, A.D. Hanlon, N. Karthik, S. Mukherjee, P. Petreczky, P. Scior et al., *Pion distribution amplitude at the physical point using the leading-twist expansion of the quasi-distribution-amplitude matrix element*, *Phys. Rev. D* **106** (2022) 074505 [2206.04084].
- [15] X.-Y. Han, J. Hua, X. Ji, C.-D. Lü, W. Wang, J. Xu et al., *A new method to access heavy meson lightcone distribution amplitudes from first-principle*, 2403.17492.
- [16] A. Khodjamirian, T. Mannel and M. Melcher, *Kaon distribution amplitude from QCD sum rules*, *Phys. Rev. D* **70** (2004) 094002 [hep-ph/0407226].
- [17] A.P. Bakulev, S.V. Mikhailov and N.G. Stefanis, *QCD based pion distribution amplitudes confronting experimental data*, *Phys. Lett. B* **508** (2001) 279 [hep-ph/0103119].
- [18] P. Ball, V.M. Braun and A. Lenz, *Twist-4 distribution amplitudes of the  $K^*$  and phi mesons in QCD*, *JHEP* **08** (2007) 090 [0707.1201].
- [19] A. Khodjamirian, R. Mandal and T. Mannel, *Inverse moment of the  $B_s$ -meson distribution amplitude from QCD sum rule*, *JHEP* **10** (2020) 043 [2008.03935].
- [20] M. Rahimi and M. Wald, *QCD sum rules for parameters of the  $B$ -meson distribution amplitudes*, *Phys. Rev. D* **104** (2021) 016027 [2012.12165].
- [21] T. Feldmann, P. Lüghausen and N. Seitz, *Strange-quark mass effects in the  $B_s$  meson's light-cone distribution amplitude*, *JHEP* **08** (2023) 075 [2306.14686].
- [22] V.M. Braun, Y. Ji and A.N. Manashov, *Higher-twist  $B$ -meson Distribution Amplitudes in HQET*, *JHEP* **05** (2017) 022 [1703.02446].
- [23] M. Beneke, G. Finauri, K.K. Vos and Y. Wei, *QCD light-cone distribution amplitudes of heavy mesons from boosted HQET*, *JHEP* **09** (2023) 066 [2305.06401].
- [24] B. Almeida-Zamora, J.J. Cobos-Martínez, A. Bashir, K. Raya, J. Rodríguez-Quintero and J. Segovia, *Light-front wave functions of vector mesons in an algebraic model*, *Phys. Rev. D* **107** (2023) 074037 [2303.09581].
- [25] B. Almeida-Zamora, J.J. Cobos-Martínez, A. Bashir, K. Raya, J. Rodríguez-Quintero and J. Segovia, *Algebraic model to study the internal structure of pseudoscalar mesons with heavy-light quark content*, *Phys. Rev. D* **109** (2024) 014016 [2309.17282].
- [26] A.J. Arifi, H.-M. Choi and C.-R. Ji, *Pseudoscalar meson decay constants and distribution amplitudes up to the twist-4 in the light-front quark model*, *Phys. Rev. D* **108** (2023) 013006 [2306.08536].
- [27] H.-M. Choi and C.-R. Ji, *Distribution amplitudes and decay constants for ( $\pi$ ,  $K$ ,  $\rho$ ,  $K^*$ ) mesons in light-front quark model*, *Phys. Rev. D* **75** (2007) 034019 [hep-ph/0701177].
- [28] C.-W. Hwang, *Analyses of decay constants and light-cone distribution amplitudes for  $s$ -wave heavy meson*, *Phys. Rev. D* **81** (2010) 114024 [1003.0972].
- [29] N. Dhiman, H. Dahiya, C.-R. Ji and H.-M. Choi, *Twist-2 Pseudoscalar and Vector Meson Distribution Amplitudes in Light-Front Quark Model with Exponential-type Confining Potential*, *Phys. Rev. D* **100** (2019) 014026 [1902.09160].
- [30] L. Chang, I.C. Cloet, J.J. Cobos-Martínez, C.D. Roberts, S.M. Schmidt and P.C. Tandy, *Imaging dynamical chiral symmetry breaking: pion wave function on the light front*, *Phys. Rev. Lett.* **110** (2013) 132001 [1301.0324].
- [31] F. Gao, L. Chang, Y.-X. Liu, C.D. Roberts and S.M. Schmidt, *Parton distribution amplitudes of light vector mesons*, *Phys. Rev. D* **90** (2014) 014011 [1405.0289].

- [32] C. Shi, L. Chang, C.D. Roberts, S.M. Schmidt, P.C. Tandy and H.-S. Zong, *Flavour symmetry breaking in the kaon parton distribution amplitude*, *Phys. Lett. B* **738** (2014) 512 [[1406.3353](#)].
- [33] C. Shi, C. Chen, L. Chang, C.D. Roberts, S.M. Schmidt and H.-S. Zong, *Kaon and pion parton distribution amplitudes to twist-three*, *Phys. Rev. D* **92** (2015) 014035 [[1504.00689](#)].
- [34] M. Ding, F. Gao, L. Chang, Y.-X. Liu and C.D. Roberts, *Leading-twist parton distribution amplitudes of S-wave heavy-quarkonia*, *Phys. Lett. B* **753** (2016) 330 [[1511.04943](#)].
- [35] B.L. Li, L. Chang, F. Gao, C.D. Roberts, S.M. Schmidt and H.S. Zong, *Distribution amplitudes of radially-excited  $\pi$  and K mesons*, *Phys. Rev. D* **93** (2016) 114033 [[1604.07415](#)].
- [36] B.-L. Li, L. Chang, M. Ding, C.D. Roberts and H.-S. Zong, *Leading-twist distribution amplitudes of scalar- and vector-mesons*, *Phys. Rev. D* **94** (2016) 094014 [[1608.04749](#)].
- [37] D. Binosi, L. Chang, M. Ding, F. Gao, J. Papavassiliou and C.D. Roberts, *Distribution Amplitudes of Heavy-Light Mesons*, *Phys. Lett. B* **790** (2019) 257 [[1812.05112](#)].
- [38] F.E. Serna, R.C. da Silveira, J.J. Cobos-Martínez, B. El-Bennich and E. Rojas, *Distribution amplitudes of heavy mesons and quarkonia on the light front*, *Eur. Phys. J. C* **80** (2020) 955 [[2008.09619](#)].
- [39] Y. Lu, D. Binosi, M. Ding, C.D. Roberts, H.-Y. Xing and C. Xu, *Distribution amplitudes of light diquarks*, *Eur. Phys. J. A* **57** (2021) 115 [[2103.03960](#)].
- [40] F.E. Serna, R.C. da Silveira and B. El-Bennich,  *$D^*$  and  $D_s^*$  distribution amplitudes from Bethe-Salpeter wave functions*, *Phys. Rev. D* **106** (2022) L091504 [[2209.09278](#)].
- [41] C. Shi, P. Liu, Y.-L. Du and W. Jia, *Heavy flavor-asymmetric pseudoscalar mesons on the light front*, *Phys. Rev. D* **110** (2024) 094010 [[2409.05098](#)].
- [42] C.D. Roberts and A.G. Williams, *Dyson-Schwinger equations and their application to hadronic physics*, *Prog. Part. Nucl. Phys.* **33** (1994) 477 [[hep-ph/9403224](#)].
- [43] P. Maris, C.D. Roberts and P.C. Tandy, *Pion mass and decay constant*, *Phys. Lett. B* **420** (1998) 267 [[nucl-th/9707003](#)].
- [44] P. Maris and C.D. Roberts, *Pi- and K meson Bethe-Salpeter amplitudes*, *Phys. Rev. C* **56** (1997) 3369 [[nucl-th/9708029](#)].
- [45] P. Maris and P.C. Tandy, *Bethe-Salpeter study of vector meson masses and decay constants*, *Phys. Rev. C* **60** (1999) 055214 [[nucl-th/9905056](#)].
- [46] P. Maris and C.D. Roberts, *Dyson-Schwinger equations: A Tool for hadron physics*, *Int. J. Mod. Phys. E* **12** (2003) 297 [[nucl-th/0301049](#)].
- [47] C.D. Roberts, M.S. Bhagwat, A. Holl and S.V. Wright, *Aspects of hadron physics*, *Eur. Phys. J. ST* **140** (2007) 53 [[0802.0217](#)].
- [48] L. Chang, Y.-x. Liu, C.D. Roberts, Y.-m. Shi, W.-m. Sun and H.-s. Zong, *Chiral susceptibility and the scalar Ward identity*, *Phys. Rev. C* **79** (2009) 035209 [[0812.2956](#)].
- [49] S.-x. Qin, L. Chang, Y.-x. Liu, C.D. Roberts and D.J. Wilson, *Interaction model for the gap equation*, *Phys. Rev. C* **84** (2011) 042202 [[1108.0603](#)].
- [50] J. Rodriguez-Quintero, *On the massive gluon propagator, the PT-BFM scheme and the low-momentum behaviour of decoupling and scaling DSE solutions*, *JHEP* **01** (2011) 105 [[1005.4598](#)].



- [51] S.-x. Qin, L. Chang, Y.-x. Liu, C.D. Roberts and D.J. Wilson, *Investigation of rainbow-ladder truncation for excited and exotic mesons*, *Phys. Rev. C* **85** (2012) 035202 [[1109.3459](#)].
- [52] P. Qin, S.-x. Qin and Y.-x. Liu, *Heavy-light mesons beyond the ladder approximation*, *Phys. Rev. D* **101** (2020) 114014 [[1912.05902](#)].
- [53] Y.-Z. Xu, C. Shi, X.-T. He and H.-S. Zong, *Chiral crossover transition from the Dyson-Schwinger equations in a sphere*, *Phys. Rev. D* **102** (2020) 114011 [[2009.12035](#)].
- [54] Y.-Z. Xu, S.-X. Qin and H.-S. Zong, *Chiral symmetry restoration and properties of Goldstone bosons at finite temperature\**, *Chin. Phys. C* **47** (2023) 033107 [[2106.13592](#)].
- [55] R.C. da Silveira, F.E. Serna and B. El-Bennich, *Strong two-meson decays of light and charmed vector mesons*, *Phys. Rev. D* **107** (2023) 034021 [[2211.16618](#)].
- [56] Y.-Z. Xu, D. Binosi, Z.-F. Cui, B.-L. Li, C.D. Roberts, S.-S. Xu et al., *Elastic electromagnetic form factors of vector mesons*, *Phys. Rev. D* **100** (2019) 114038 [[1911.05199](#)].
- [57] M. Chen and L. Chang, *A pattern for the flavor dependent quark-antiquark interaction*, *Chin. Phys. C* **43** (2019) 114103 [[1903.07808](#)].
- [58] Q. Li, C.-H. Chang, T. Wang and G.-L. Wang, *Strong decays of  $P_{\psi}^N(4312)^+$  to  $J/\psi(\eta_c)p$  and  $\bar{D}^{(*)}\Lambda_c$  within the Bethe-Salpeter framework*, *JHEP* **06** (2023) 189 [[2301.02094](#)].
- [59] Y.-Z. Xu, M. Ding, K. Raya, C.D. Roberts, J. Rodríguez-Quintero and S.M. Schmidt, *Pion and kaon electromagnetic and gravitational form factors*, *Eur. Phys. J. C* **84** (2024) 191 [[2311.14832](#)].
- [60] Y.-Z. Xu, *The electromagnetic form factors of heavy-light pseudo-scalar and vector mesons*, *JHEP* **07** (2024) 118 [[2402.06141](#)].
- [61] F.E. Serna, B. El-Bennich and G.a. Krein, *Parton distribution functions and transverse momentum dependence of heavy mesons*, *Phys. Rev. D* **110** (2024) 114033 [[2409.01441](#)].
- [62] M.A. Sultan, J. Kang, A. Bashir and L. Chang, *Neutral pion to two-photons transition form factor revisited*, *Phys. Rev. D* **110** (2024) 114047 [[2409.09595](#)].
- [63] Y.-Z. Xu and K. Raya, *The  $D^*D\pi$  and  $B^*B\pi$  couplings from Dyson-Schwinger equations framework*, [2411.12327](#).
- [64] K. Raya, A. Bashir and J. Rodríguez-Quintero, *Mapping spatial distributions within pseudoscalar mesons*, [2412.06025](#).
- [65] A.S. Miramontes, K. Raya, A. Bashir, P. Roig and G. Paredes-Torres, *Radially excited pion: electromagnetic form factor and the box contribution to the muon's  $g - 2$* , [2411.02218](#).
- [66] C. Chen, F. Gao and S.-x. Qin, *Screening masses of positive- and negative-parity hadron ground-states, including those with strangeness*, [2412.15045](#).
- [67] F. Gao, A.S. Miramontes, J. Papavassiliou and J.M. Pawłowski, *Heavy-light mesons from a flavour-dependent interaction*, [2411.19680](#).
- [68] Z.N. Xu, Z.Q. Yao, D. Binosi, M. Ding, C.D. Roberts and J. Rodríguez-Quintero, *Distribution Functions of a Radially Excited Pion*, [2501.13243](#).
- [69] LHCb collaboration, *Test of lepton universality using  $B^+ \rightarrow K^+\ell^+\ell^-$  decays*, *Phys. Rev. Lett.* **113** (2014) 151601 [[1406.6482](#)].

- [70] LHCb collaboration, *Angular analysis of the  $B^0 \rightarrow K^{*0} \mu^+ \mu^-$  decay using  $3 \text{ fb}^{-1}$  of integrated luminosity*, *JHEP* **02** (2016) 104 [[1512.04442](#)].
- [71] LHCb collaboration, *Test of lepton universality with  $B^0 \rightarrow K^{*0} \ell^+ \ell^-$  decays*, *JHEP* **08** (2017) 055 [[1705.05802](#)].
- [72] R. Mukundan, S. Ong and P. Lee, *Image analysis by tchebichef moments*, *IEEE Transactions on Image Processing* **10** (2001) 1357.
- [73] A. Townsend and L.N. Trefethen, *An extension of chebfun to two dimensions*, *SIAM Journal on Scientific Computing* **35** (2013) C495.
- [74] T. Hahn, *CUBA: A Library for multidimensional numerical integration*, *Comput. Phys. Commun.* **168** (2005) 78 [[hep-ph/0404043](#)].
- [75] T. Hahn, *Concurrent Cuba*, *J. Phys. Conf. Ser.* **608** (2015) 012066 [[1408.6373](#)].
- [76] J. Berntsen, T.O. Espelid and A. Genz, *An adaptive algorithm for the approximate calculation of multiple integrals*, *ACM Trans. Math. Softw.* **17** (1991) 437–451.
- [77] J. Berntsen, T.O. Espelid and A. Genz, *Algorithm 698: Dcuhre: an adaptive multidimensional integration routine for a vector of integrals*, *ACM Trans. Math. Softw.* **17** (1991) 452–456.
- [78] M.B. Hecht, C.D. Roberts and S.M. Schmidt, *Valence quark distributions in the pion*, *Phys. Rev. C* **63** (2001) 025213 [[nucl-th/0008049](#)].
- [79] D. Binosi, L. Chang, J. Papavassiliou and C.D. Roberts, *Bridging a gap between continuum-QCD and ab initio predictions of hadron observables*, *Phys. Lett. B* **742** (2015) 183 [[1412.4782](#)].
- [80] Y.-Z. Xu, S. Chen, Z.-Q. Yao, D. Binosi, Z.-F. Cui and C.D. Roberts, *Vector-meson production and vector meson dominance*, *Eur. Phys. J. C* **81** (2021) 895 [[2107.03488](#)].
- [81] C.S. Fischer, P. Watson and W. Cassing, *Probing unquenching effects in the gluon polarisation in light mesons*, *Phys. Rev. D* **72** (2005) 094025 [[hep-ph/0509213](#)].
- [82] E. Rojas, B. El-Bennich and J.P.B.C. de Melo, *Exciting flavored bound states*, *Phys. Rev. D* **90** (2014) 074025 [[1407.3598](#)].
- [83] M. Blank, *Properties of quarks and mesons in the Dyson-Schwinger/Bethe-Salpeter approach*, Ph.D. thesis, Graz U., 2011. [1106.4843](#).
- [84] H. Sanchis-Alepuz and R. Williams, *Recent developments in bound-state calculations using the Dyson-Schwinger and Bethe-Salpeter equations*, *Comput. Phys. Commun.* **232** (2018) 1 [[1710.04903](#)].
- [85] PARTICLE DATA GROUP collaboration, *Review of Particle Physics*, *Phys. Rev. D* **98** (2018) 030001.
- [86] CLEO collaboration, *Study of B decays to charmonium states  $B \rightarrow \eta(c) K$  and  $B \rightarrow \chi(c0) K$* , *Phys. Rev. Lett.* **86** (2001) 30 [[hep-ex/0007012](#)].
- [87] N. Mathur, M. Padmanath and S. Mondal, *Precise predictions of charmed-bottom hadrons from lattice QCD*, *Phys. Rev. Lett.* **121** (2018) 202002 [[1806.04151](#)].
- [88] K. Cichy, M. Kalinowski and M. Wagner, *Continuum limit of the D meson,  $D_s$  meson and charmonium spectrum from  $N_f = 2 + 1 + 1$  twisted mass lattice QCD*, *Phys. Rev. D* **94** (2016) 094503 [[1603.06467](#)].

- [89] R.J. Dowdall, C.T.H. Davies, T.C. Hammant and R.R. Horgan, *Precise heavy-light meson masses and hyperfine splittings from lattice QCD including charm quarks in the sea*, *Phys. Rev. D* **86** (2012) 094510 [[1207.5149](#)].
- [90] Z. Fu and L. Wang, *Studying the  $\rho$  resonance parameters with staggered fermions*, *Phys. Rev. D* **94** (2016) 034505 [[1608.07478](#)].
- [91] HADRON SPECTRUM collaboration, *Resonances in coupled  $\pi K - \eta K$  scattering from quantum chromodynamics*, *Phys. Rev. Lett.* **113** (2014) 182001 [[1406.4158](#)].
- [92] HPQCD collaboration,  *$V_{cs}$  from  $D_s \rightarrow \phi \ell \nu$  semileptonic decay and full lattice QCD*, *Phys. Rev. D* **90** (2014) 074506 [[1311.6669](#)].
- [93] ETM collaboration, *Masses and decay constants of  $D_{(s)}^*$  and  $B_{(s)}^*$  mesons with  $N_f = 2 + 1 + 1$  twisted mass fermions*, *Phys. Rev. D* **96** (2017) 034524 [[1707.04529](#)].
- [94] G.C. Donald, C.T.H. Davies, R.J. Dowdall, E. Follana, K. Hornbostel, J. Koponen et al., *Precision tests of the  $J/\psi$  from full lattice QCD: mass, leptonic width and radiative decay rate to  $\eta_c$* , *Phys. Rev. D* **86** (2012) 094501 [[1208.2855](#)].
- [95] HPQCD, UKQCD collaboration, *High Precision determination of the  $\pi$ ,  $K$ ,  $D$  and  $D(s)$  decay constants from lattice QCD*, *Phys. Rev. Lett.* **100** (2008) 062002 [[0706.1726](#)].
- [96] C. McNeile, C.T.H. Davies, E. Follana, K. Hornbostel and G.P. Lepage, *Heavy meson masses and decay constants from relativistic heavy quarks in full lattice QCD*, *Phys. Rev. D* **86** (2012) 074503 [[1207.0994](#)].
- [97] A. Bazavov et al.,  *$B$ - and  $D$ -meson leptonic decay constants from four-flavor lattice QCD*, *Phys. Rev. D* **98** (2018) 074512 [[1712.09262](#)].
- [98] B. Colquhoun, R.J. Dowdall, C.T.H. Davies, K. Hornbostel and G.P. Lepage,  *$\Upsilon$  and  $\Upsilon'$  Leptonic Widths,  $a_\mu^b$  and  $m_b$  from full lattice QCD*, *Phys. Rev. D* **91** (2015) 074514 [[1408.5768](#)].
- [99] HPQCD collaboration,  *$B$ -meson decay constants: a more complete picture from full lattice QCD*, *Phys. Rev. D* **91** (2015) 114509 [[1503.05762](#)].
- [100] F.E. Serna, B. El-Bennich and G.a. Krein, *Charmed mesons with a symmetry-preserving contact interaction*, *Phys. Rev. D* **96** (2017) 014013 [[1703.09181](#)].
- [101] M.A. Ivanov, Y.L. Kalinovsky and C.D. Roberts, *Survey of heavy meson observables*, *Phys. Rev. D* **60** (1999) 034018 [[nucl-th/9812063](#)].
- [102] M. Gómez-Rocha, T. Hilger and A. Krassnigg, *Effects of a dressed quark-gluon vertex in vector heavy-light mesons and theory average of the  $B_c^*$  meson mass*, *Phys. Rev. D* **93** (2016) 074010 [[1602.05002](#)].
- [103] S.-X. Qin and C.D. Roberts, *Resolving the Bethe–Salpeter Kernel*, *Chin. Phys. Lett.* **38** (2021) 071201 [[2009.13637](#)].
- [104] M. Blank and A. Krassnigg, *Matrix algorithms for solving (in)homogeneous bound state equations*, *Comput. Phys. Commun.* **182** (2011) 1391 [[1009.1535](#)].
- [105] K. Glau, D. Kressner and F. Statti, *Low-rank tensor approximation for chebyshev interpolation in parametric option pricing*, *SIAM Journal on Financial Mathematics* **11** (2020) 897 [[1902.04367](#)].
- [106] A. Markowsky and N. Schopohl, *Cold bose atoms around the crossing of quantum waveguides*, *Phys. Rev. A* **89** (2014) 013622 [[1309.3205](#)].

- [107] B. Bahr, G. Rabuffo and S. Steinhaus, *Renormalization of symmetry restricted spin foam models with curvature in the asymptotic regime*, *Phys. Rev. D* **98** (2018) 106026 [[1804.00023](#)].
- [108] M. Longton, *Time-Symmetric Rolling Tachyon Profile*, *JHEP* **09** (2015) 111 [[1505.00802](#)].
- [109] A. Kapustin, B. Willett and I. Yaakov, *Tests of Seiberg-like dualities in three dimensions*, *JHEP* **08** (2020) 114 [[1012.4021](#)].
- [110] G. Bell and T. Feldmann, *Modelling light-cone distribution amplitudes from non-relativistic bound states*, *JHEP* **04** (2008) 061 [[0802.2221](#)].